NAVAL POSTGRADUATE SCHOOL
Monterey, California

THESIS

Statistical Characterization of Graphite Fiber for Prediction of Composite Structure Reliability

by

Carl Robert Engelbert

June 1990

Thesis Advisor Professor Edward M. Wu

Unclassified

Security Classification of this page

REPORT DOCUMENTATION PAGE

1a Report Security Classification Unclassified	1b Restrictive Markings
2a Security Classification Authority	3 Distribution Availability of Report
2b Declassification/Downgrading Schedule	Approved for public release; distribution is unlimited.
4 Performing Organization Report Number(s)	5 Monitoring Organization Report Number(s)
6a Name of Performing Organization Naval Postgraduate School	6b Office Symbol (If Applicable) 67
6c Address (city, state, and ZIP code) Monterey, CA 93943-5000	7a Name of Monitoring Organization Naval Postgraduate School
8a Name of Funding/Sponsoring Organization	8b Office Symbol (If Applicable)
8c Address (city, state, and ZIP code)	7b Address (city, state, and ZIP code) Monterey, CA 93943-5000
	9 Procurement Instrument Identification Number
	10 Source of Funding Numbers

Program Element Number	Project No	Task No	Work Unit Accession No

11 Title (Include Security Classification) Statistical Characterization of Graphite Fiber for Prediction of Composite Structure Reliability

12 Personal Author(s) Carl R. Engelbert, LCDR USN

13a Type of Report	13b Time Covered From To	14 Date of Report (year, month,day)	15 Page Count
Master's Thesis		June 1990	89

16 Supplementary Notation The views expressed in this thesis are those of the author and do not reflect the official policy or position of the Department of Defense or the U.S. Government.

17 Cosati Codes			18 Subject Terms (continue on reverse if necessary and identify by block number)
Field	Group	Subgroup	Graphite fiber strength testing, Graphite fiber statistical evaluation, *continued on reverse*

19 Abstract (continue on reverse if necessary and identify by block number

ABSTRACT

The increased use of composite materials in Navy Applicatons brings with it the need to know quantitatively the reliability of composite structures. Traditional methods of reliability prediction cannot be used. Therefore, analytical modeling is required, and experimental methods with which to assess the model are needed. This research refined experimental methods and obtained benchmark statistical data on the strength of graphite fibers. With the Chain-of-Bundles local load sharing model, the data were then used as a guide to perform a parametric influence study on the sensitivity of composite structure reliability to the statistical distribution of its constituent graphite fibers. The results indicate a strong influence by the lower tail of the single fiber statistical distribution, which has important implications for design, acceptance testing, and other Navy procurement functions.

20 Distribution/Availability of Abstract	21 Abstract Security Classification
[X] unclassified/unlimited [ ] same as report [ ] DTIC users	Unclassified

22a Name of Responsible Individual	22b Telephone (Include Area code)	22c Office Symbol
Edward M. Wu	(408) 646-3459	67

DD FORM 1473, 84 MAR 83 APR edition may be used until exhausted

All other editions are obsolete

security classification of this page Unclassified

[18] Composite reliability predictions

Approved for public release; distribution is unlimited.

Statistical Characterization of Graphite Fiber for Prediction of Composite Structure Reliability

by

Carl Robert Engelbert
Lieutenant Commander, United States Navy
BBA, University of Wisconsin, 1974

Submitted in partial fulfillment of the requirements for the degree of

MASTER OF SCIENCE IN AERONAUTICAL ENGINEERING

from the

NAVAL POSTGRADUATE SCHOOL
June 1990

Author: Carl R. Engelbert
Carl Robert Engelbert

Approved by: Edward M. Wu
Edward M. Wu, Thesis Advisor

Gerald H. Lindsey
Gerald H. Lindsey, Second Reader

E.R. Wood
E.R. Wood, Chairman,
Department of Aeronautics and Astronautics

ABSTRACT

The increased use of composite materials in Navy applications brings with it the need to know quantitatively the reliability of composite structures. Traditional methods of reliability prediction cannot be used. Therefore, analytical modeling is required, and experimental data with which to assess the model are needed. This research refined experimental methods and obtained benchmark statistical data on graphite fibers. With the Chain-of-Bundles local load sharing model, the data were then used as a guide to perform a parametric influence study on the sensitivity of composite structure reliability to the statistical distribution of its constituent graphite fibers. The results indicate a strong influence by the lower tail of the single fiber statistical distribution, which has important implications for design, acceptance testing, and other Navy procurement functions.

TABLE OF CONTENTS

ACKNOWLEDGMENTS

It is only fitting at the outset to thank those people who made this thesis possible. First and foremost, I wish to thank my wife, Maureen. Her constant support and understanding made it possible to keep going, through thick and thin. She has the patience of a saint and the strength enough for both of us. I couldn't have done it without her. Our children did their part too, and for their encouragement and sacrifices I thank them.

In the lab, this research could not have happened without Jim Nageotte. His technical expertise and astute observations often were the key to getting past stumbling blocks along the way. But it was his quiet dedication that made the difference. Over two thirds of the data reported on here were patiently and carefully recorded by Jim. That's a lot of work.

Finding the words to thank Professor Wu is not easy. He cared enough that when I asked for a fish, he refused to give one. Instead, he taught me how to fish. It was his enormous effort that made it possible for me to do much of this work myself, and for that I will always be grateful. In the truest sense of the word, he gave me an education.

I. INTRODUCTION

The use of composite materials in Navy and national security related applications has grown from its early status of specialized applications only, where cost was no object, to the current status of many large volume applications. Composite materials consist of strong, stiff fibers embedded in a typically ductile matrix binder. Composites are advantageous over homogeneous materials (steel, aluminum, titanium, etc) in many applications because they are strong, lightweight, corrosion resistant, and their directional nature permits optimizing design for maximum efficiency.

A not so commonly recognized advantage is the micro-redundancy inherent in composites. Micro-redundancy results from fiber elements in parallel at the microscopic level such that when one element fails, other elements continue to carry the load. Some structures can be designed with macro-redundancy by adding additional spars, ribs, stiffener plates, etc. For other inherently monolithic structures, (pressure vessels, for example) macro-redundancy can not be achieved. For such applications, micro-redundancy must be explored, and when fully understood, exploited.

Table I presents examples of Navy applications (some in use, others in design), along with their relative sizes given in spools of fiber required for composite fabrication. A spool is a packaging unit consisting of typically two to five pounds of fiber. Reliability is crucial for each application, as loss of life is almost certain if catastrophic composite failure occurs. Reliability also influences cost, resource allocation, maintenance schedules, and logistics. As new designs (aircraft, ships, satellites, etc) are planned with longer service lives than in the past, reliability

TABLE I

Structure	Spools
Pilot ejection seat flask	1
Submarine air flask	75
A-6 Wing	500
Submarine Hull	5000

predictions become increasingly important. Under-estimation of reliability penalizes structural performance. Over-estimation of reliability will cause unacceptably high failure rates prior to the end of planned service, resulting in costly fixes, loss of defense capability, or both. Therefore, it is imperative to know the quantitative reliability of a structure before it is built.

A. RELIABILITY DETERMINATION

Reliability is the probability that a given article will not fail under a given set of conditions. There are essentially three methods of determining reliability: experience, direct testing, or analytical modeling (i.e. mathematical characterization). Whereas reliability of materials has traditionally been determined through the first two methods, their applicability to composites must to be reexamined.

1. Experience

Experience cannot be used because typically, the particular composite for a new application does not even exist until six months to a year prior to prototype fabrication. Additionally, improved fibers are continually being developed and merely changing the fiber type in a given composite can drastically change its reliability.

2. Direct testing

Likewise, direct testing is impractical. Direct testing generally requires a sample size one order of magnitude larger than desired reliability (e.g. for 10^5 reliability, 10^6 specimens are required). Direct testing obviously cannot be implemented for structures such as those listed in Table I. Analytical modeling is left as the only alternative then.

3. Analytical modeling

Analytical modeling can be either experience based or probabilistic based. Experience based modeling uses an empirical cumulative distribution function (ECDF) directly without fitting a function to the historical data. With extensive data an ECDF is as good as, or better than, a good model. On the other hand, probabilistic modeling is either ad hoc (an equation is used to achieve the best fit to sufficient data) or physically based, which requires an understanding of the failure process itself. Because data for composites are not available and cannot be acquired in a timely manner, physically based modeling is the only alternative.

The analytical model based on current understanding of composite failure under uniaxial tension is described in the next chapter. The essence of this model is that composite failure is directly related to fiber strength and variability characteristics. Therefore a model that describes failure in a single fiber is needed

as a basis for the model of the composite. The generally accepted single fiber model is also described in the next chapter. This investigation examines analytically and experimentally the premise that if the statistics of the constituent fiber are known, then the probability of composite failure can be analytically predicted.

B. EXPERIMENTAL PROCEDURES

Given that fiber statistics are at the ground level in composite reliability predictions, explicit procedures must be defined by which data can be collected *uncolored* by experimental implementation. The capability to obtain uncolored fiber statistics is essential for two reasons:

- Model development stage: Fiber statistics are correlatable to composite statistics through the analytical model. Both uncolored fiber statistics and uncolored composite statistics are required before the adequacy of the model can be assessed.
- Model application stage: Once confirmed, the analytical model will be used to predict composite reliability. The prediction can only be as good as the fiber statistics used, so again uncolored fiber statistics are required.

The test methodology and techniques developed in the laboratory are, then, extremely important. Eventually they can be transformed into industrial quality control procedures through technology transfer initiatives. Meanwhile, the Navy must develop expertise in this area to enable enlightened specification drafting, acceptance testing, and many other procurement functions.

C. SCOPE OF THIS INVESTIGATION

The primary goal of this investigation was to acquire uncolored fiber statistics from carefully refined, executed, and documented experimental procedures which

would provide a benchmark for assessing the adequacy of the current composite reliability model.

Concurrently, numerical calculations using the analytical model were performed to predict composite reliability. A reasonable range of values for the single fiber shape parameter was used to perform a parametric influence analysis. The sensitivity of composite reliability to fiber parameters is important not only because of its impact on specifications and acceptance testing, but also because it can direct the focus of research and development efforts. For example, strong influence by both tails of the fiber distribution has one set of implications while strong influence by the lower tail and weak influence by the upper tail has another, and so on.

II. BACKGROUND

Mathematical characterization of the composite failure process requires models at two levels; a single fiber model and a local load sharing model, that describes the micro-redundancy, in order to relate fiber strength statistics to composite reliability.

A. SINGLE FIBER MODEL

Graphite fibers are typically packaged in the form of continuous strands wrapped on spools. A strand consists of 1,000 to 10,000 individual filaments, each about eight microns in diameter. The exact number of filaments in a strand varies and is optimized based on the manufacturing technology and the specific application. Throughout this investigation, the term fiber is used to mean a single filament rather than a strand.

Fiber failure under tension is understood to result from pre-existing flaws in the fiber. Weibull [Ref. 1] proposed that for many materials, the statistical distribution of *severity* and *location* of such flaws determines its failure characteristics. This lead to the "weakest link" rule; that catastrophic failure occurs when stress at any one flaw exceeds the ability of the surrounding material to halt crack propagation. Weibull derived the following expression to describe the weakest link distribution:

$$F(x) = 1-\exp\left\{-\left(\frac{x}{\beta}\right)^{\alpha}\right\} \tag{2.1}$$

where

F(x) = failure probability under applied load

x = applied load

α = shape parameter

β = scale parameter

The Weibull model is generally accepted to represent a single fiber, with a Poisson spatial distribution of flaws along its length. A fiber can be thought of, then, as many segments in *series*, with fiber strength governed by the weakest segment.

Weibull probability paper is generally used to plot the cumulative distribution function (CDF) for fiber statistics. Algebraic operations on equation 2.1 leads to the different, equivalent form:

$$\ln(-\ln[1-F(x)])=\alpha \ln(x) -\alpha \ln \beta.$$

If we let $F^* = \ln(-\ln[1-F(x)])$

then $F^* = \alpha \ln(x) + \text{constant}$ (2.2)

Equation 2.2 is seen to be the equation of a line on Weibull probability paper which is linear in ln(x) on the abcissa and linear in F* on the ordinate .

Figure 1 shows a typical Weibull plot, with scales in F(x) and x provided for comparison. Weibull probability paper is also very useful for displaying *size* effect phenomena associated with the weakest link rule. The CDF for n elements in series, $F_n(x)$, is simply F(x) translated vertically by the amount ln(n), as shown in Figure 1.

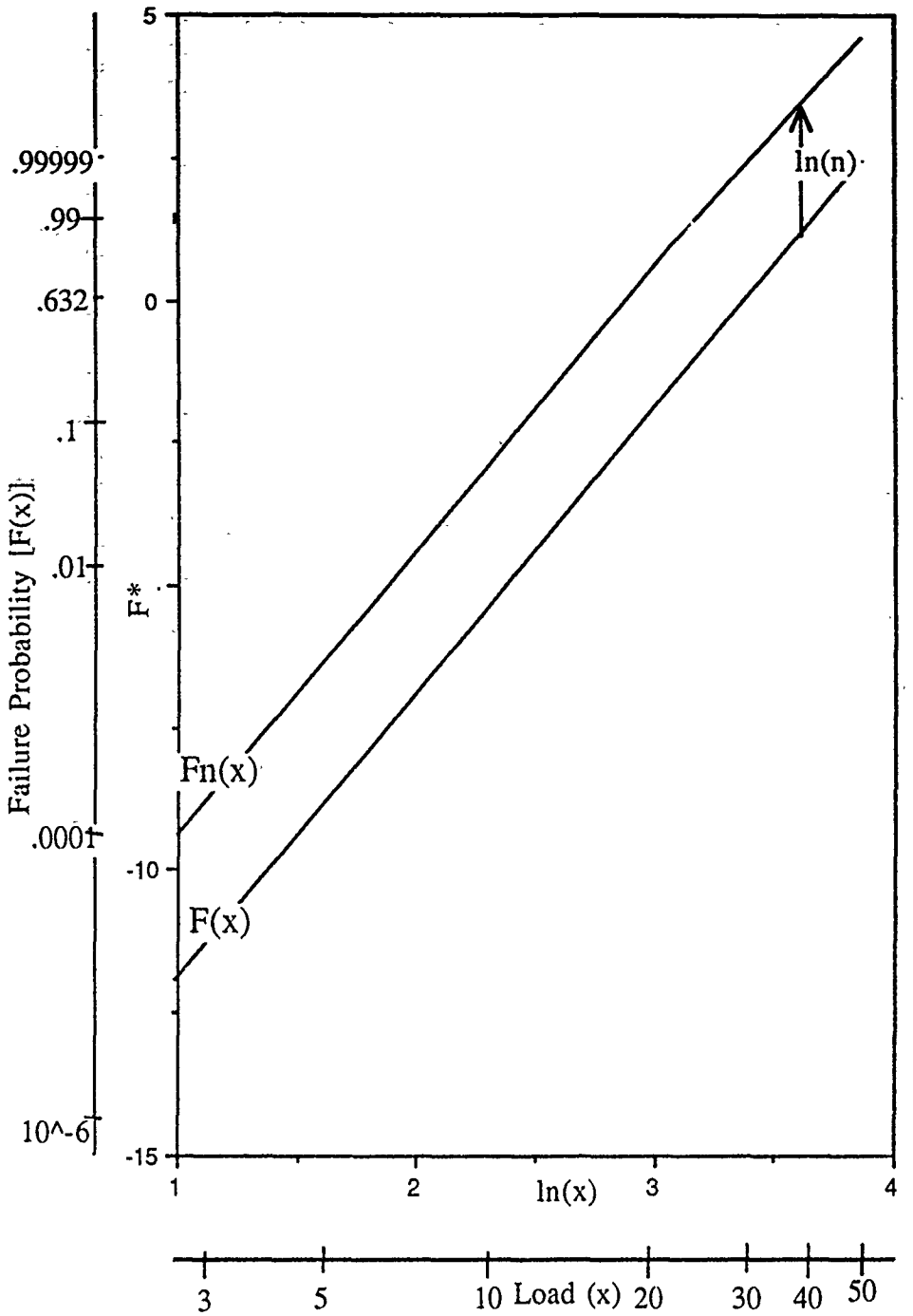

Figure 1. Weibull Linear Behavior

B. MODE SHAPES

Weibull probability paper is also very useful for revealing deviations from Weibull linear behavior. This is important to an open issue with fiber statistics; whether they are uni-modal or multi modal. Figure 2 compares uni-modal with multi-modal behavior. From the physical understanding of the fiber failure process, it can be deduced that if experimental data follow uni-modal behavior, then only one origin, or cause, of flaws exists. Conversely, multi-modal behavior, as observed by Metcalfe and Schmitz in their work with glass fibers [Ref. 2], infers the existence of more than one origin of flaws. The same *inference* can be made for graphite fibers, despite the physical differences from glass.

Multi-modal behavior, if observed in graphite fibers, has many implications for composite reliability, as will be shown in chapter five. For the Navy, this translates to operational implications (maintenance scheduling and logistics) as well as procurement implications (specifications and acceptance testing). Additionally, if multiple origins of flaws are determined to exist, research and development efforts may find one or more of them relatively easy to eliminate. This could bring large reductions in fiber variability, with commensurately large gains in composite reliability.

This investigation addressed the uni-modal versus multi-modal issue on two levels. At the experimental level, sufficient data were gathered to allow a meaningful interpretation of the statistical mode shape observed. These results are presented in Chapter four. At the analytical level, reliability sensitivity to fiber modality was explored through a numerical parametric sensitivity study for a variety of both uni-modal and multi-modal shapes. Parametric influence results are presented in Chapter five.

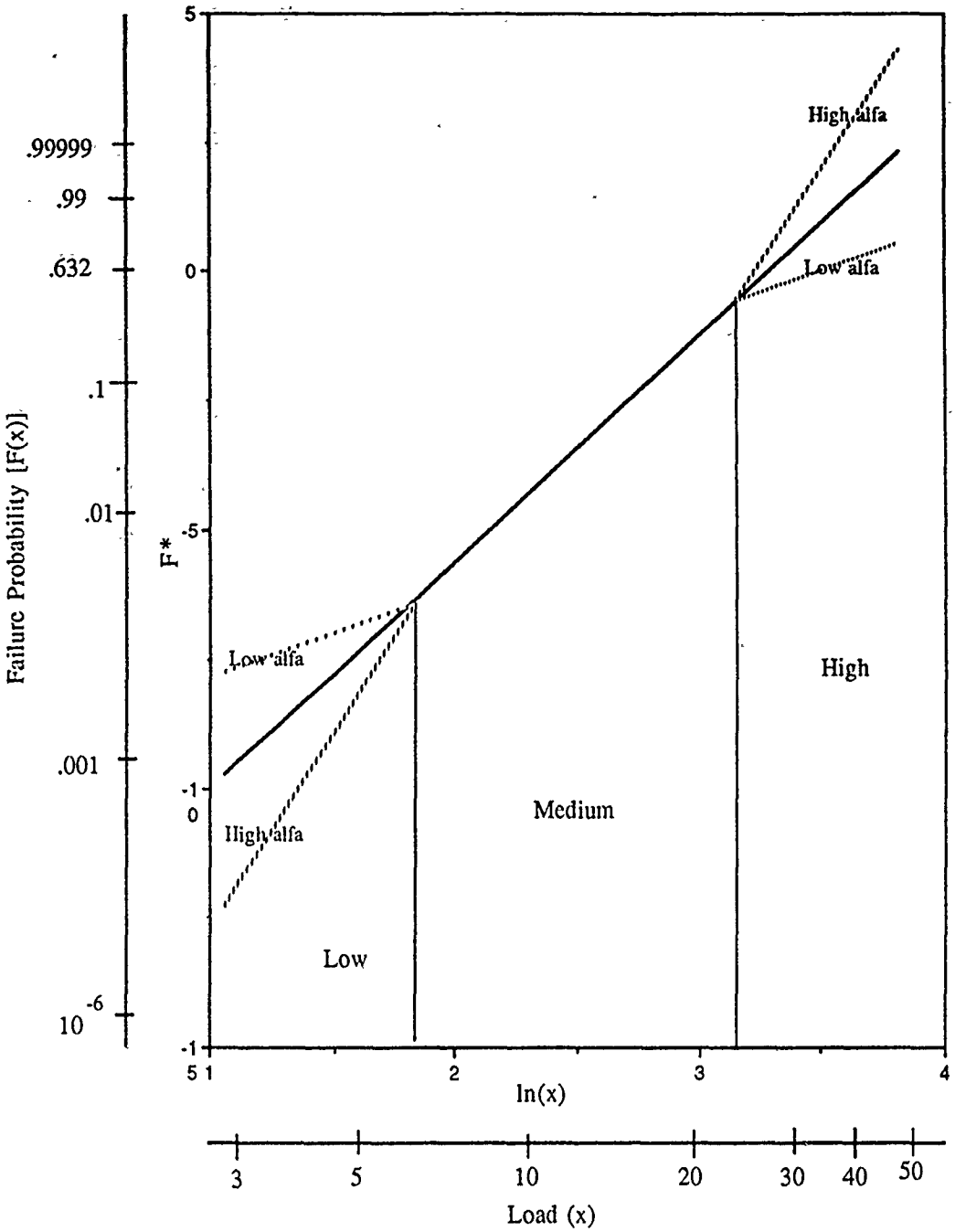

Figure 2. Uni-Modal and Multi-Modal Behavior

C. CHAIN-OF-BUNDLES MODEL

While single fibers are modeled as segments in series, with no redundancy, composite materials are known to have micro-redundancy. The Chain-of-Bundles model, proposed by Rosen [Ref. 3], accounts for micro-redundancy in relating fiber statistics to composite structure reliability. Fibers in parallel are called a bundle. A composite structure can be thought of as a chain of bundles, with the fibers in each bundle imbedded in an epoxy matrix. In tension, the entire load is considered to be equally shared by the fibers. Upon failure of a single fiber, its share of the load is transferred to surviving fibers by the matrix through shear. Current understanding of composite fracture is based on failure in sequence as follows:

- Fibers fail under applied load as a result of statistically distributed flaws.
- Weakest fiber failures are initiated at very low loads.
- Load is transferred to surviving fibers, thereby preventing catastrophic macroscopic failure.
- As external load increases, additional weak fibers fail. Stress concentrations at the initial failure sites lead to failure site clustering.
- The largest cluster site causes the most severe stress concentration, which ultimately leads to catastrophic failure of the structure.

1. Load Sharing Rule

Assumptions about the physical process of load transfer after individual fibers break is a central issue in the analytical model. Historically two different load sharing rules have been used. The Equal Load Sharing rule (ELS) developed by Daniel [Ref. 4] assumes that all surviving fibers equally share the load

previously carried by a failed fiber. This rule is most relevant in modeling wires and cables. However, for a structural composite with a matrix binder present, the Local Load Sharing rule (LLS) developed in varying versions by Zweben and Rosen [Ref. 5], Harlow and Phoenix [Ref. 6], and others, is more realistic. The LLS rule assumes that the immediate neighbors of a failed fiber bear most of the shifted load, and that distant neighbors bear almost none.

2. Chain-of-Bundles Refinement

Mathematical refinement of the Chain-of-Bundles model by Harlow and Phoenix [Ref. 7], permits the numerical calculation of a benchmark relation between fiber statistics and composite failure probability. In their version, the model is restricted to bundles whose fibers are arranged in a circular array with equal spacing. This is a mathematical convenience that allows load factors to be calculated for all possible configurations of failed and surviving fibers, while capturing the essence of the composite failure process with key features that are believed to persist for other geometries as well. Mathematical formulations are provided that account for all possible combinations and permutations of fiber failure configurations during sequential failure. The steps required for the formulations are:

- All possible *states* of failed and surviving fibers are accounted for.
- Load factors for each state are generated according to the LLS.
- All possible failure *sequences* are generated.
- The probability of each sequence occurring is generated. These probabilities depend on single fiber statistics.
- The probabilities for all sequences are summed to obtain overall probability of composite structure failure at a given load.
- The process is then repeated for various loads over the range of interest.

These mathematical formulations were used in the parametric influence study conducted as part of this investigation, reported on in Chapter five.

III. FIBER STRENGTH TEST METHOD

While the first two chapters elucidated the necessity for fiber statistics *uncolored* by experimental implementation, this chapter reports on the careful refinement and execution of experimental procedures that were used to obtain data considered uncolored. The tests were conducted in the NPS Advanced Composites Laboratory using the NPS integrated test system (NPSITS). This system enables semi-automated measurement of fiber diameter through laser diffraction techniques, followed by tensile loading to failure, with a minimum of sample handling which is a known source of coloring to the data. Figure 3 depicts a fiber mounted for diameter measurement and tensile testing, figure 4 presents a schematic of the NPSITS diameter measuring system and figure 5 presents a schematic of the NPSITS tensile testing system.

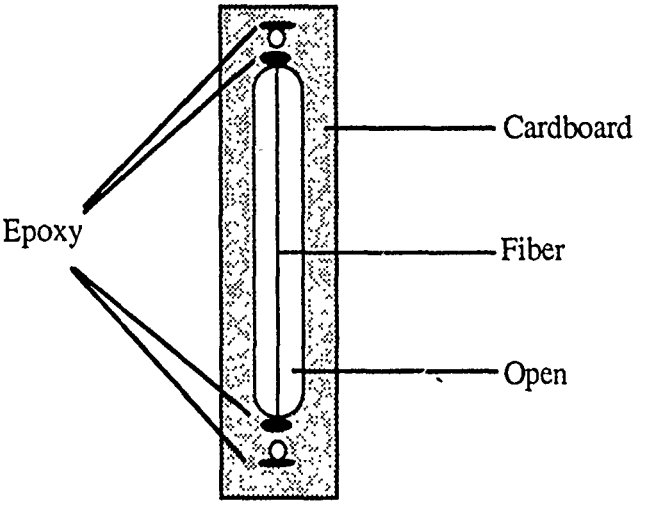

Figure 3. Fiber Sample Mounted For Testing

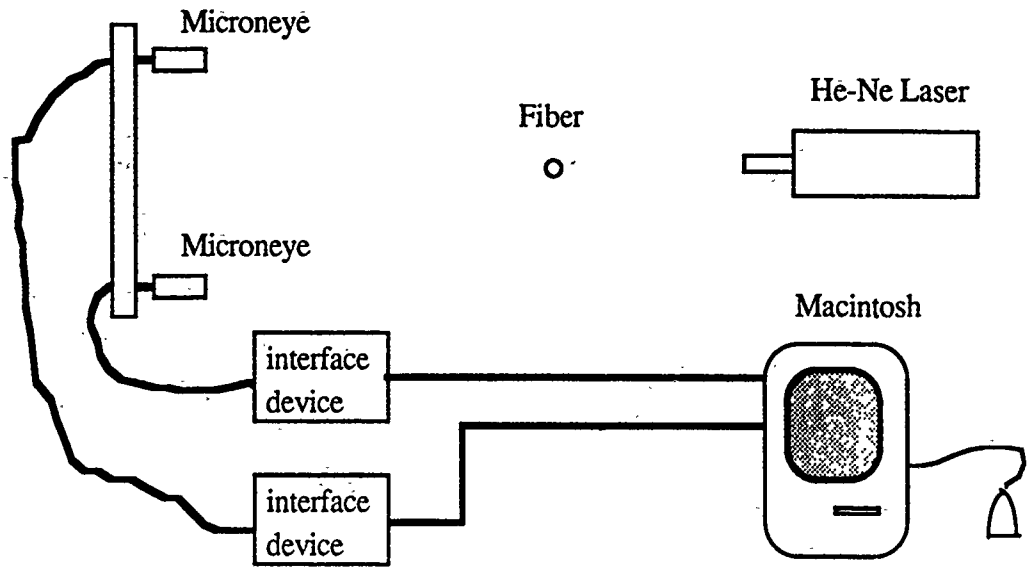

Figure 4. Schematic of NPSITS Diameter Measuring System

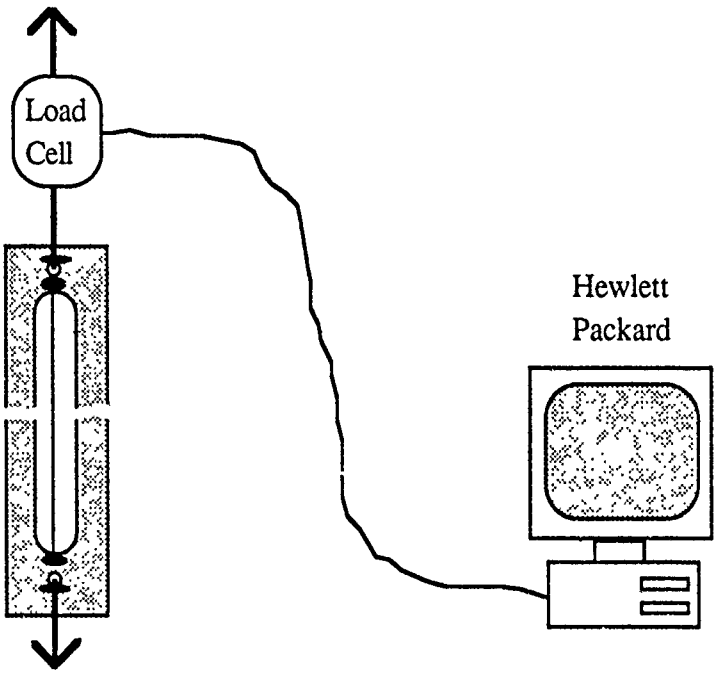

Figure 5. Schematic of NPSITS Tensile Testing System

A. TEST METHOD OVERVIEW

Data were recorded on samples from two different spools of Hercules AS4 graphite fiber strands (AS4-008 and AS4-019). Samples were 50 mm in gauge length, and were tested in accordance with standard ASTM procedures. Tests were conducted by two different operators. In order to build proficiency, approximately 75 practice samples were constructed by each operator prior to actual testing. Learning curve phenomena were observed initially, so the intent was to proceed beyond the steep part of the learning curve prior to recording any data. Numerous handling techniques were explored during this stage to find the method with the least potential for damaging the fiber samples.

Three hundred and twenty nine total data points were recorded (AS4-008: 167 points, AS4-019: 162 points). Tests were conducted in batches of approximately 20 samples each, over an eight month period. Batch by batch comparisons for each operator were conducted to determine if learning curve phenomena were still present. No evidence of learning curve influence was found; that is, the measured strength for latter batches shown neither an increase in mean strength nor a decrease in variability. Batches were also compared between operators to insure that operator-dependent differences did not exist. Again no evidence of bias was found.

Testing consisted of two separate phases. In the first phase, a batch of samples was prepared and stored. This phase contained the greatest potential for damage to the fibers. The second phase consisted of measuring the fiber's diameter, followed by a monotonically increasing tension until failure. Normal laboratory care in

handling test specimens was considered sufficient in this phase to prevent fiber sample damage.

A detailed description of sample preparation methods and handling precautions is contained in Appendix A. A detailed description of diameter measurement methods is contained in Appendix B.

B. TEST INSTRUMENTATION

Instrumentation used in testing was carefully evaluated and calibrated to reduce uncertainty in the data. A load cell in series with the fiber under tension was used to record failure load. The load cell was calibrated, using weight standards and Interactive Data Acquisition Software (IDAS) [Ref. 8], prior to and after each test, and at regular intervals during extended test sessions. The laser diffraction equipment used to measure fiber diameter required significant operator interaction, but demonstrated exceptional repeatability. Diameter measurements made on the NPSITS, compared with measurements made by scanning electron microscopy (SEM), were found to produce similar results (See Appendix B). Mechanical compliance testing, using zero-gauge-length samples, was also conducted to determine the amount of the *recorded* sample elongation that was attributable to instrumentation and test procedures (e.g. hysteresis, taking up slack, slippage, etc.). This "compliance" could then be subtracted from recorded elongation data to increase the accuracy of strain data.

C. MAJOR CONCERNS

Two significant sources of bias to the data were identified:x

- Fiber samples not selected at random.
- Fibers damaged prior to test.

Non-random selection of test samples would result from inadvertent, de facto proof testing. Proof testing refers to placing material specimens under a predetermined load to intentionally break the weak ones, leaving only proven strong ones for structural use. Merely the process of extracting an eight micron filament (approximately one fifth the size of a human hair) from a strand of up to ten thousand filaments, if not done with extreme care, is sure to break the weak ones. The result would be to bias the data towards higher loads.

Fibers damaged during sample preparation subsequent to fiber extraction, but prior to testing, would produce the opposite bias. Weakened fibers would be tested, biasing the data towards lower loads. Interaction of the two sources of bias may cancel one another, but there is no way to be certain of that. Therefore, this investigation devised methods of avoiding these sources of potential errors. The first source was relatively easy to guard against. The second source was more difficult for two reasons:

- It is physically impossible to extract fibers without *some* damage (i.e. the process can only make the fibers weaker, never stronger).
- Many potential sources of damage to fibers exist, all of which had to be accounted for.

Appendix A details the procedures used to avoid inadvertent proof testing and contains a list of damage modes identified, along with steps taken to avoid them.

D. PARAMETER ESTIMATION

Single fiber statistical parameters must be estimated from experimental data. Uncertainty in parameter estimation can be caused by random, externally-caused error due to the testing process. Measures taken to reduce uncertainty from this

source were discussed in the previous section. Parameter uncertainty also arises from the random intrinsic strength *resolution*, which is dependent on the number of samples tested. This is addressed in chapter four.

A third source of uncertainty arises from the method used for parameter estimation. The Maximum Likelihood Estimator method [Ref. 9], was used in this investigation. A "likelihood function", L(x, θ), is defined such that:

$$L(x,\theta) = \prod_{i=1}^{n} f(x_i,\theta)$$

where θ is the set of unknown constant parameters (in the two parameter Weibull case, the shape and scale parameters α and β) that describe the distribution of the random variable X for given data set, which consists of a set of measured values x. L (the probability of occurrence of the measured values x_i) is a function of θ, and the maximum of L(θ) is found by setting its derivatives with respect to the parameters equal to zero. The resulting values of α and β, then, have the maximum likelihood of being the "true" parameters for the underlying population, based on the sample population tested.

The Maximum Likelihood Estimator (MLE) is known to be an unbiased estimator for sample sizes greater than 100, a condition met by the data sets analyzed in this research. For smaller data sets, the MLE bias is known and can easily be accounted for. A computer spreadsheet was used in this investigation to perform the iterations necessary to obtain MLE parameter estimates.

IV. TEST RESULTS

The experimental phase results of this investigation are reported in this chapter. Graphical representation is used here while tabular data are included as Appendix C. Interpretation of the data includes: a) analysis of the empirical cumulative distribution functions (ECDF's); b) comparison of the transformed CDF's to Weibull linear behavior and investigation of mode shapes observed; c) comparison of data from the two different spools; and d) an analysis of stress versus load as the random variable.

A. TEST DATA AND PARAMETER ESTIMATION

Figures 6 and 7 present the ECDF's for AS4-008 and AS4-019 fibers respectively, plotted in untransformed coordinates of expected rank (F) versus failure load (x). Data are coded by operator for visual assessment of operator-dependent trends. A preponderance of data from one operator occurring at either extreme of strength and vice versa for the other operator would indicate a bias. Both sets show a good mix of data points from each operator over the entire range, hence no operator-dependent biases are evident. The plots also show the wide variability in fiber strength. Failure loads ranged from 2.85 gms to 25.5 gms; a complete order of magnitude difference.

Figures 8 and 9 present the AS4-008 and AS4-019 fiber data respectively, plotted on Weibull probability paper. Both sets of data exhibited substantial Weibull linear behavior, as expected based on the close match of the mathematical weakest link model to the physical configuration of a small diameter filament.

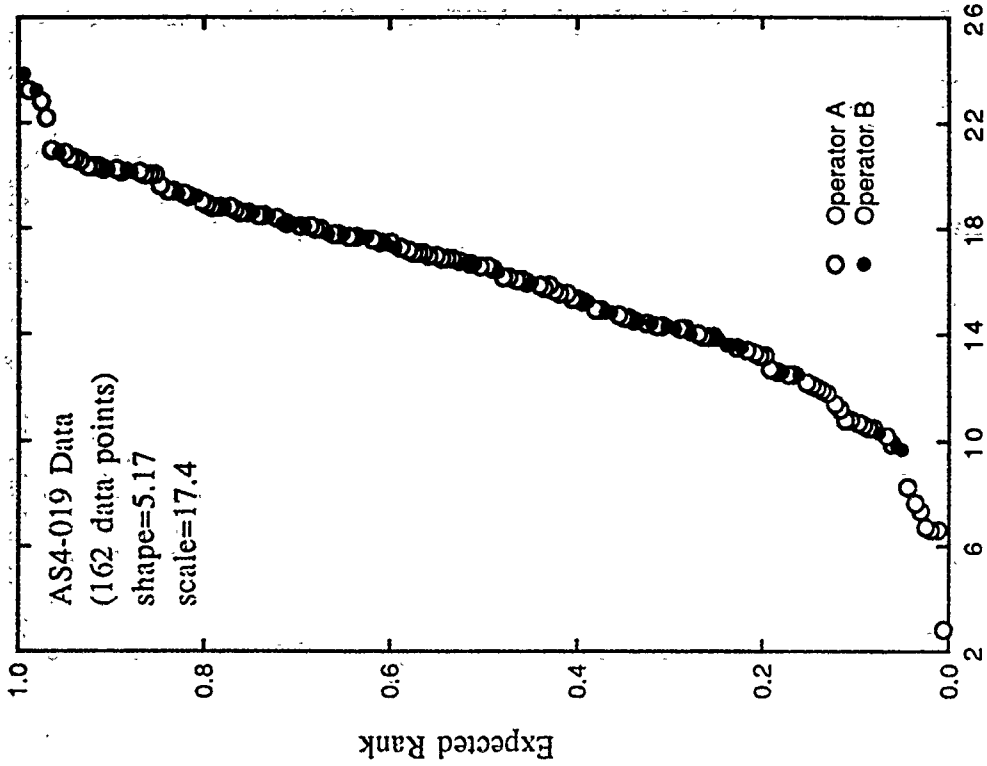

Figure 7. AS4-019 Empirical CDF

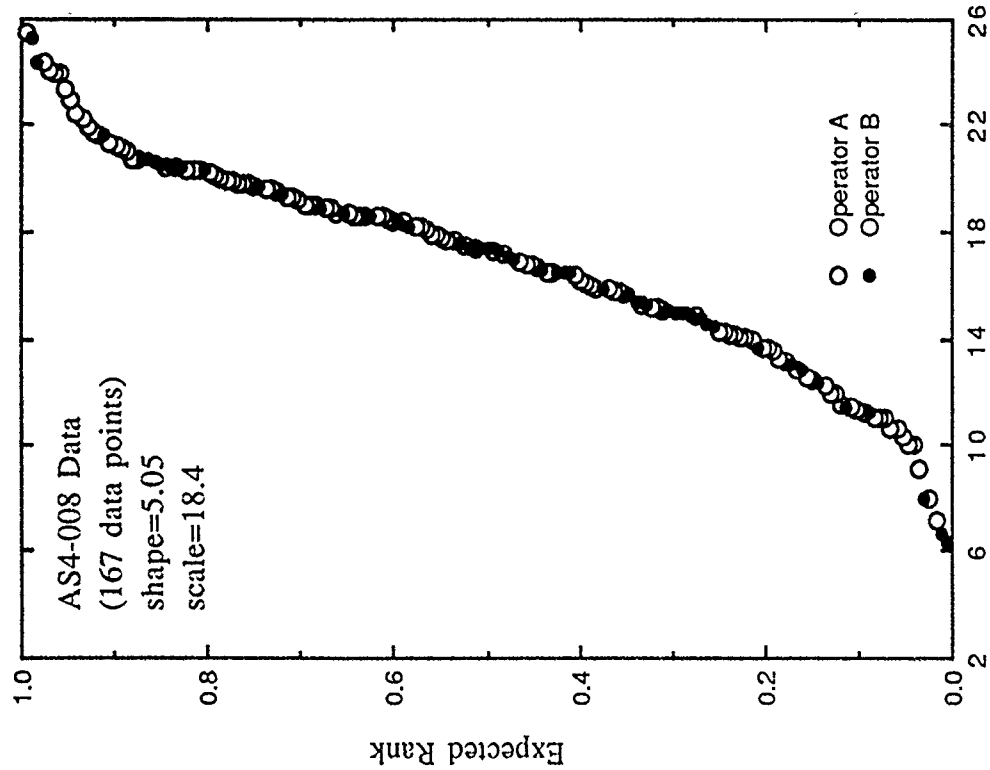

Figure 6. AS4-008 Empirical CDF

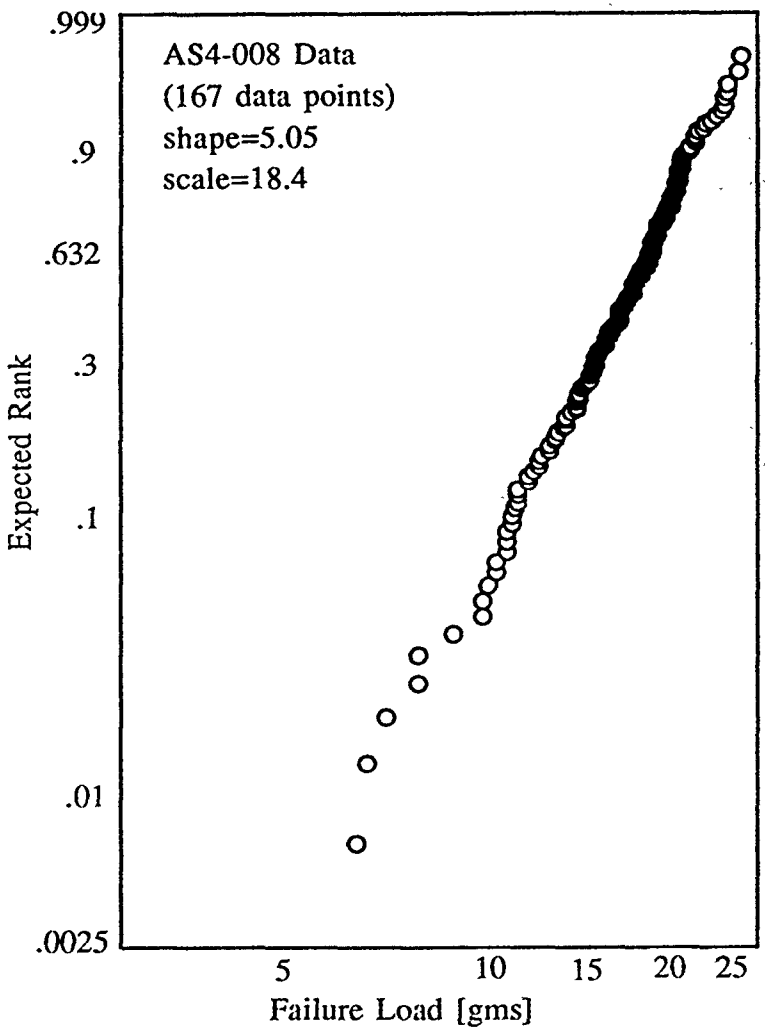

Figure 8. AS4-008 Weibull CDF

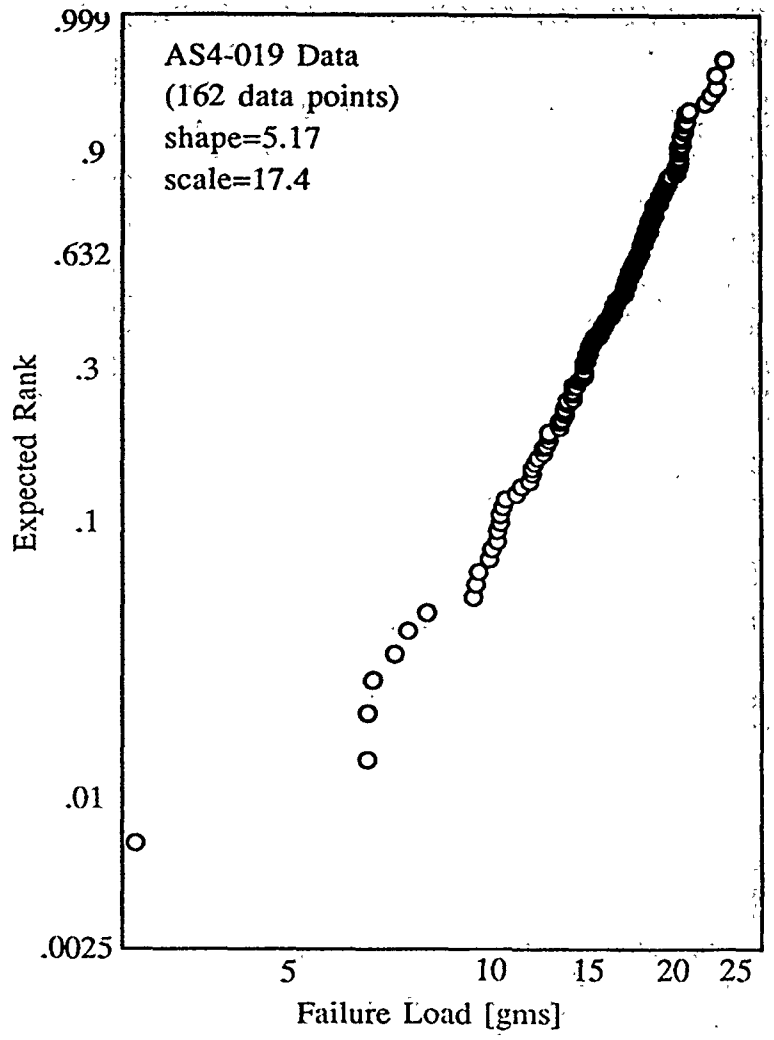

Figure 9. AS4-019 Weibull CDF

B. UNI-MODAL VERSUS MULTI-MODAL

Maximum Likelihood Estimates (MLE) of the shape and scale parameters based on the experimental data are presented in Table II. These parameters were fitted to a uni-modal two parameter Wiebull model, and therefore plot as straight lines on Weibull probability paper.

TABLE II

Parameter	AS4-008	AS4-019
Shape	5.05	5.17
Scale	18.4	17.4

Figures 10 and 11 show the estimated Weibull curves superimposed on the AS4-008 and AS4-019 data respectively. Of particular interest is the lower tail behavior for both data sets. Both lower tails show more scatter than that exhibited by data in the mid-strength range, but the scatter does not appear to be random. For random scatter, one would expect approximately the same number of points on either side of the estimated parameter line. Here, however, both lower tails consist entirely of points to the left (i.e. weak side) of the uni-modal estimated parameter. Therefore, a case could be made for a bi-modal distribution as depicted in figures 12 and 13.

These results are very important in light of the parametric influence study (chapter five) conducted as part of this investigation in which lower tail behavior was found to have a strong influence on composite reliability. That result, in

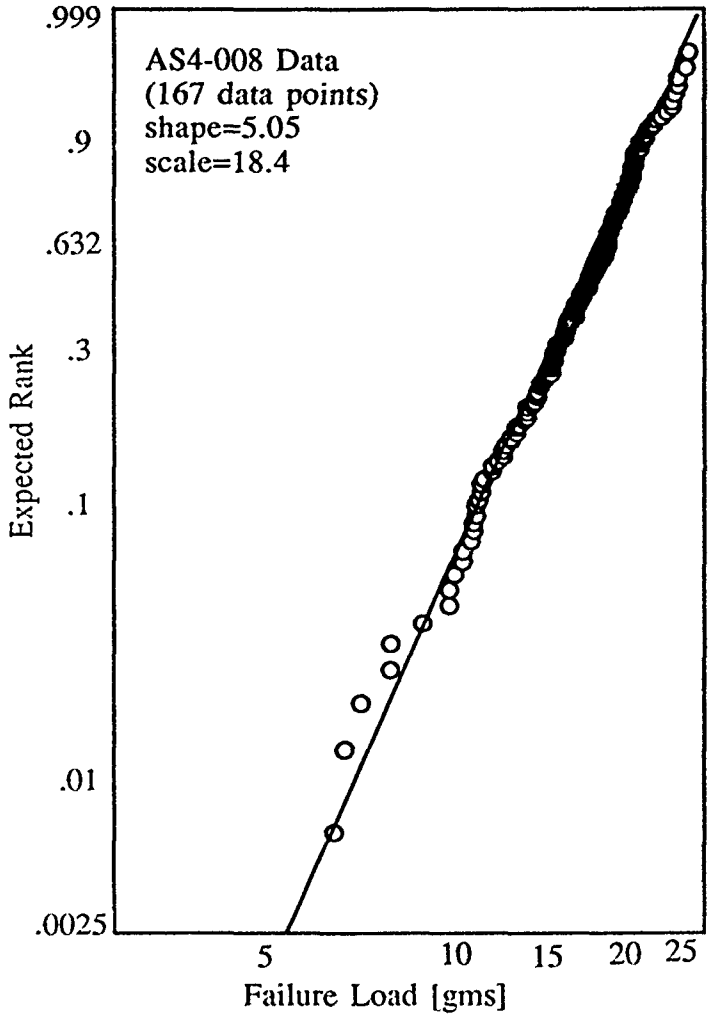

Figure 10. AS4-008 CDF With MLE Curve

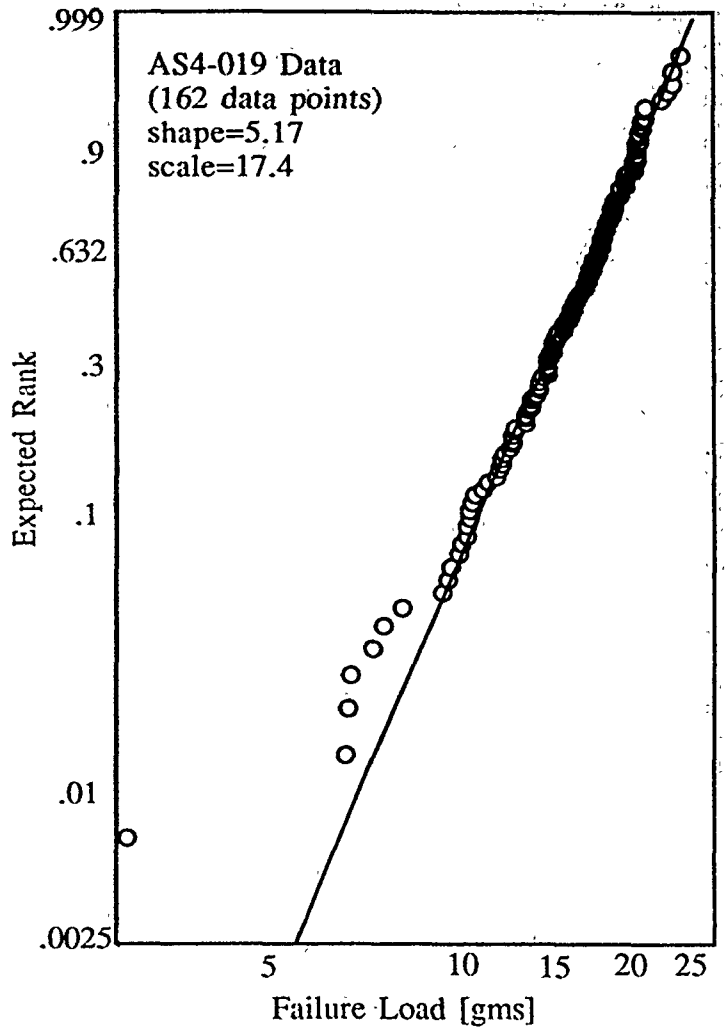

Figure 11. AS4-019 CDF With MLE Curve

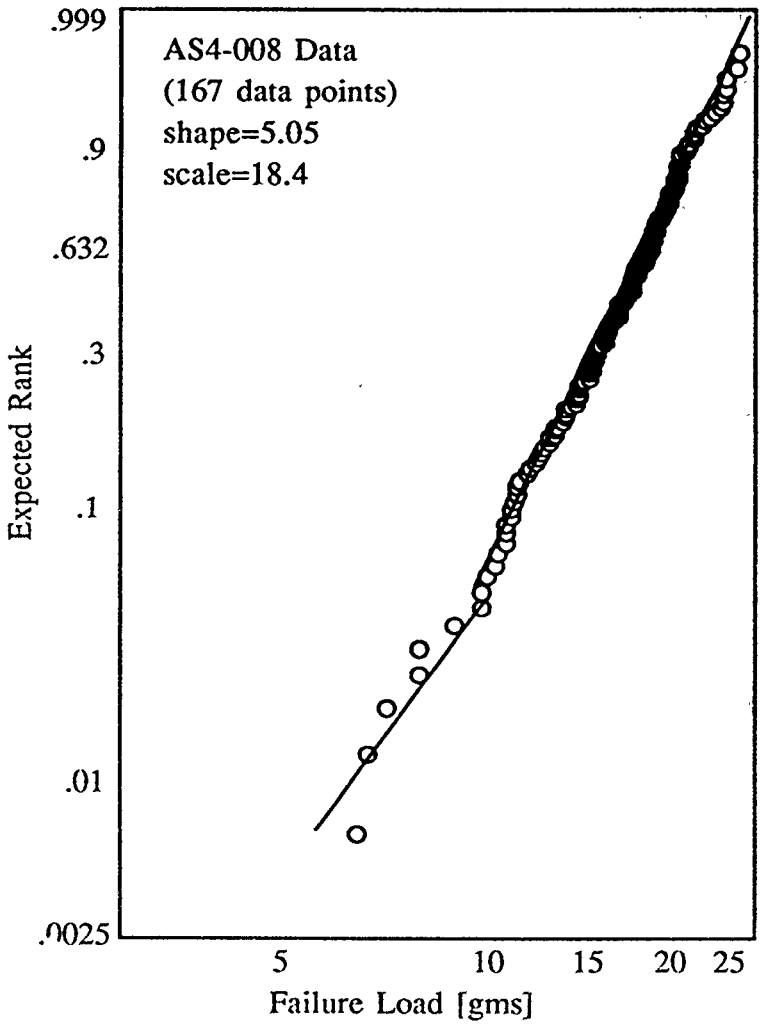

Figure 12. AS4-008 CDF (Bi-Modal)

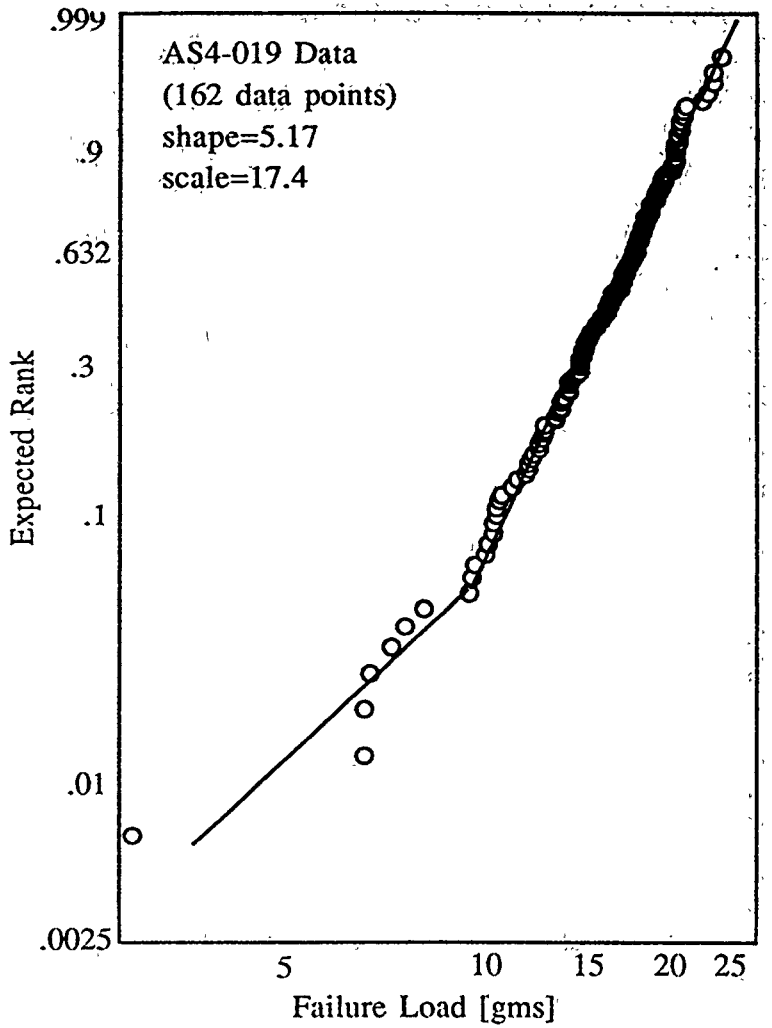

Figure 13. AS4-019 CDF (Bi-Modal)

conjunction with the observed lower tail behavior of both sets of AS4 data, indicates the need to conduct further testing. For a larger sample size the lower tail will extend further, providing a better indication of true lower tail modality.

C. TWO SPOOLS COMPARED

Given the importance of fiber statistics to composite reliability predictions, a question arises regarding the resolution possible in fiber testing. While all of the graphite fibers tested in this investigation were AS4 grade, manufactured by the same manufacturer, it was desired to know if the fibers came from the same population, statistically. Figure 14 shows both AS4-008 and AS4-019 data, without the estimated curves, while figure 15 shows only the estimated Weibull curves. Confidence interval tables exist for Weibull distributions, but only for sample sizes up to 50. For larger sample sizes, the confidence interval may be calculated [Ref. 11] from the rank (a beta distribution) through a transformation to obtain an **F** distributed random variable. This calculation was beyond the scope of this investigation.

Visually, both plots indicate that there is a significant difference in the scale parameter, and that the AS4-008 fibers are stronger. In fact, these results are consistent with the results of earlier strength tests conducted on actual composites made from the same two spools [Ref. 12]. This consistency of results gives strong evidence that fiber statistics can be used as a predictor for composite characteristics.

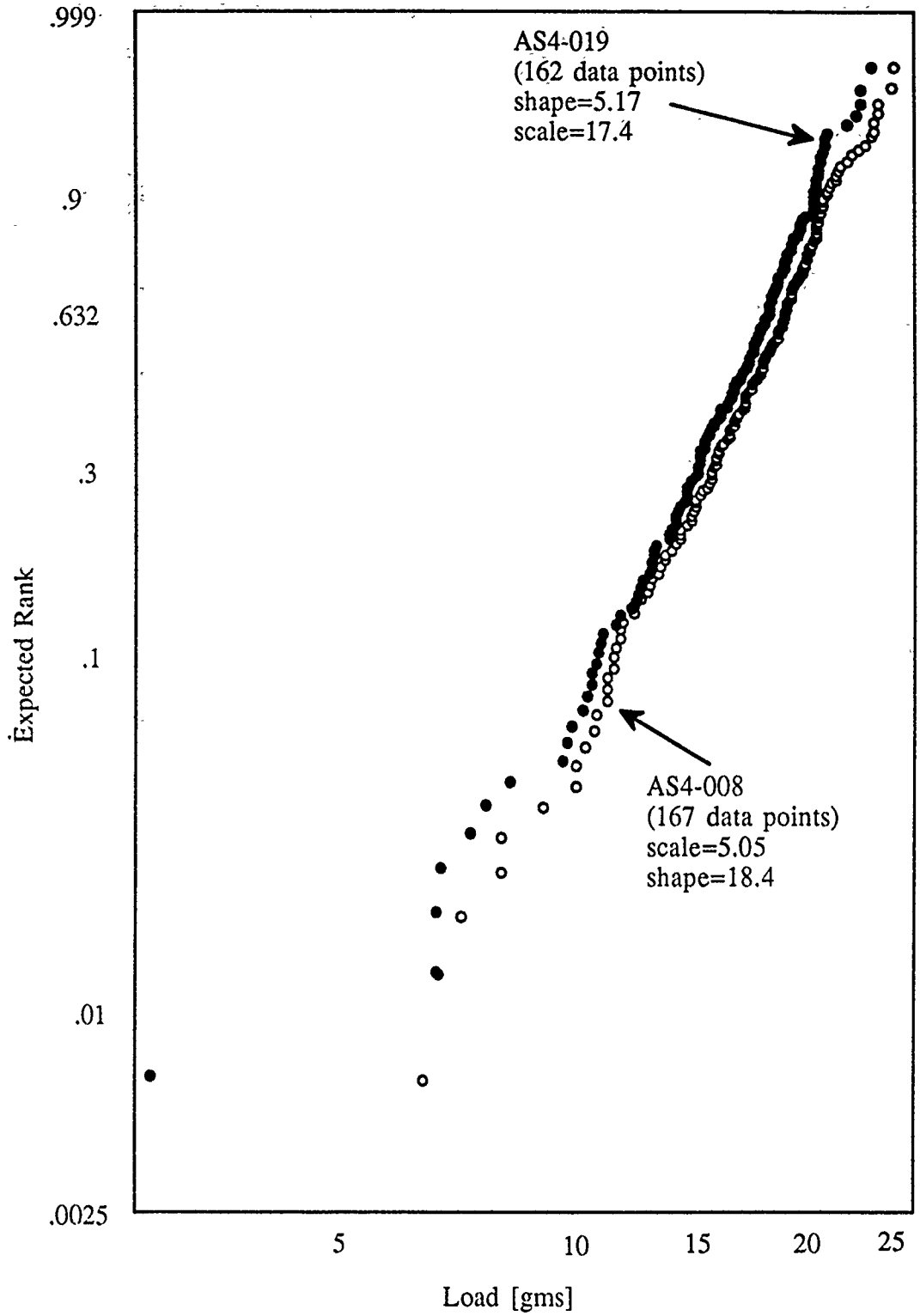

Figure 14. Data Set Comparison

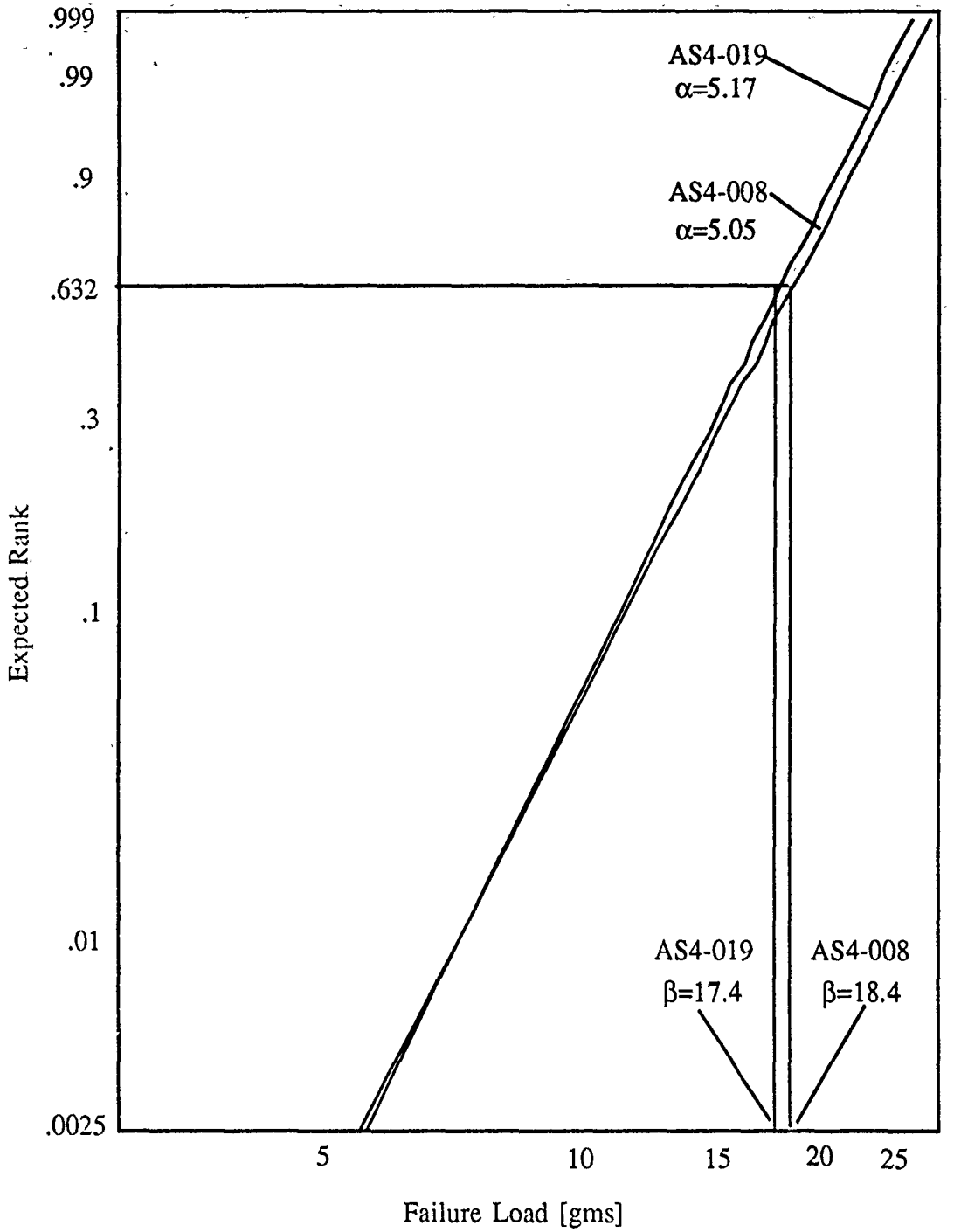

Figure 15. AS4-008 and AS4-019 MLE Curve Comparison

D. STRESS VERSUS LOAD

The choice of which random variable to use for fiber statistics must be an enlightened one. Load (or force) and stress are the two logical candidates. At issue is which one will cause fiber statistics to exhibit the greatest variability (i.e. the lowest shape parameter). Kunkel [Ref. 10] demonstrated that estimating a shape parameter higher than that of the "true" population for single fibers will result in non-conservative reliability predictions for composite structures. This situation is highly undesirable. Therefore, whichever random variable shows the greatest variability should be used for fiber statistics.

Stress is simply load divided by area. In the case of graphite fibers, both failure load and diameter (hence area) are random variables. It is known that, *if independent of each other*, the stochastic interaction of two random variables will produce more variability in a dependent property than would result from a single random variable. This effect was confirmed for the interaction of load and diameter through simulations performed by Kunkel [Ref. 10]. Therefore, if failure load and diameter are independent, stress would be expected to have more variability (i.e. lower shape parameter) than load, as the random variable for fiber statistics. To date failure load and diameter for graphite fibers have been proven neither dependent nor independent. Goeke and Chou [Ref. 13] observed no correlation in their data for AS4, IM6, and IM7 fibers, but concluded that their sample sizes were insufficient to rigorously determine independence. Sample sizes in this investigation were approximately three times the sample size of 50 used by Goeke and Chou.

Figures 16 and 17 are plots of failure load versus diameter for AS4-008 and AS4-019 data respectively. Visually there appears to be no correlation for either

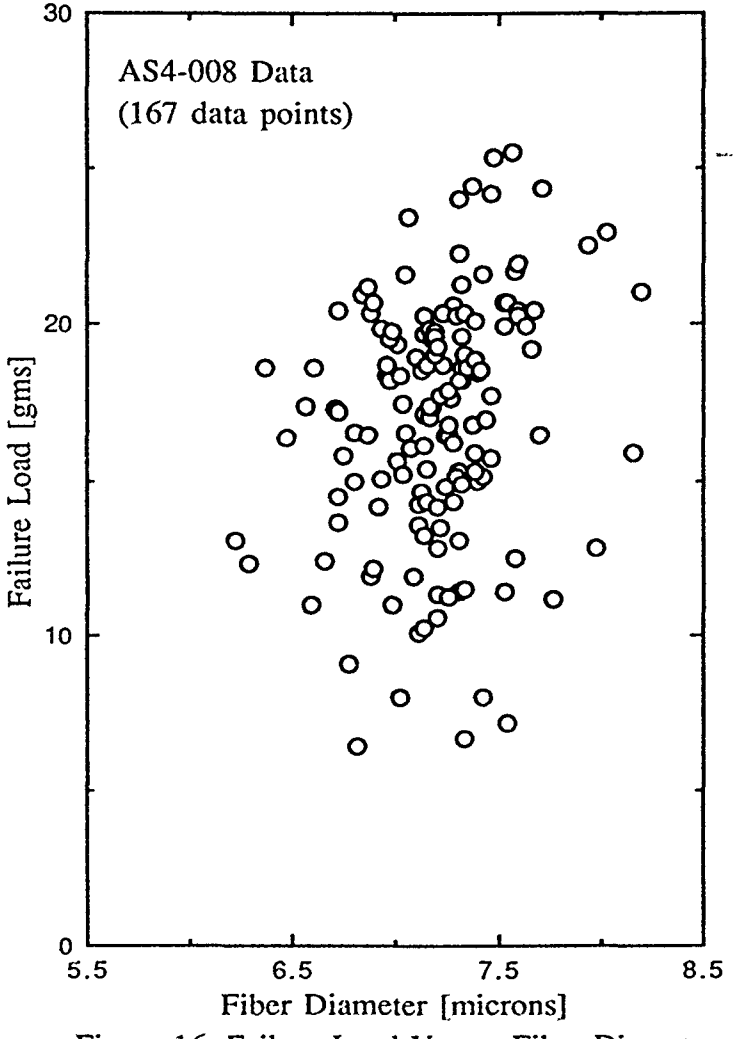

Figure 16. Failure Load Versus Fiber Diameter

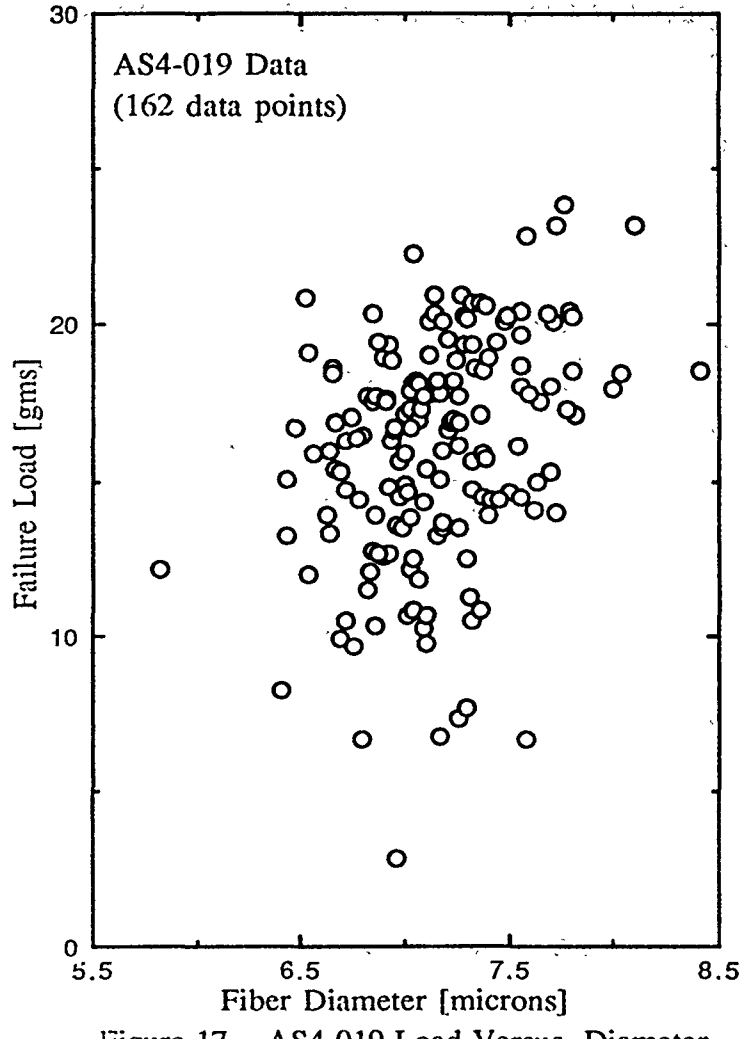

Figure 17. AS4-019 Load Versus Diameter

set of data, indicating independence of failure load and fiber diameter. One would therefore expect stress to exhibit greater variability than load as the random variable. This was investigated by calculating MLE estimates of the shape parameter using stress instead of load. These estimates are compared in Table III.

TABLE III

Spool	Shape (load)	Shape (stress)	Change
AS4-008	5.05	5.21	+3.6%
AS4-019	5.17	4.30	-16.8 %

The results are inconclusive. The shape parameter for stress is higher than that for load in one case, and lower in the other. Further testing is required.

E. MODULUS OF ELASTICITY

As a final check on the data, the load-deformation relationship was investigated. Failure load versus deformation is plotted in figure 18 for seven test samples chosen at random from the AS4-008 data. As can be seen, there is significant scatter in the failure loads, the sample deformations, and the stiffness slopes associated with each data point. This is as expected given that each sample had a different diameter (hence cross-sectional area). When the difference in cross sectional areas is accounted for, the data show consistency in the modulus of elasticity. The load-deformation slopes from figure 18 are plotted versus the corresponding fiber cross sectional areas in figure 19, along with a line depicting the slope-versus-area relationship for a constant modulus of 3.9×10^7 psi. The uniformity of modulus displayed supports the conclusions that:

- The instrumentation and procedures used faithfully measure fiber diameter characteristics.
- The observed variability in ultimate load and ultimate stress is intrinsic to the population of AS4 graphite fibers.

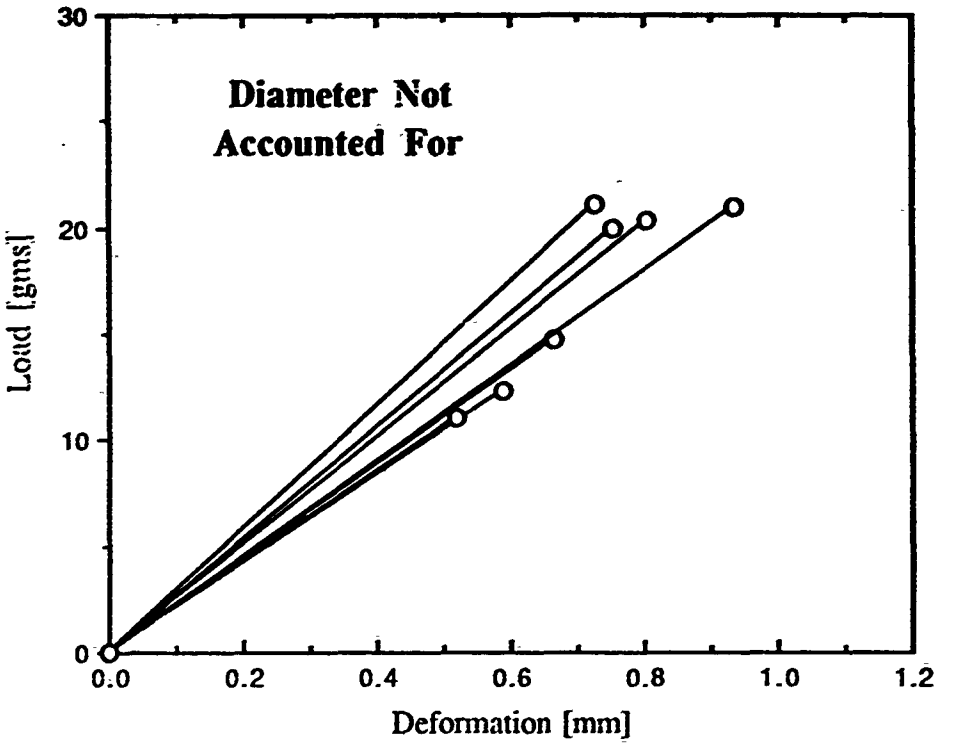

Figure 18. Load Versus Deformation

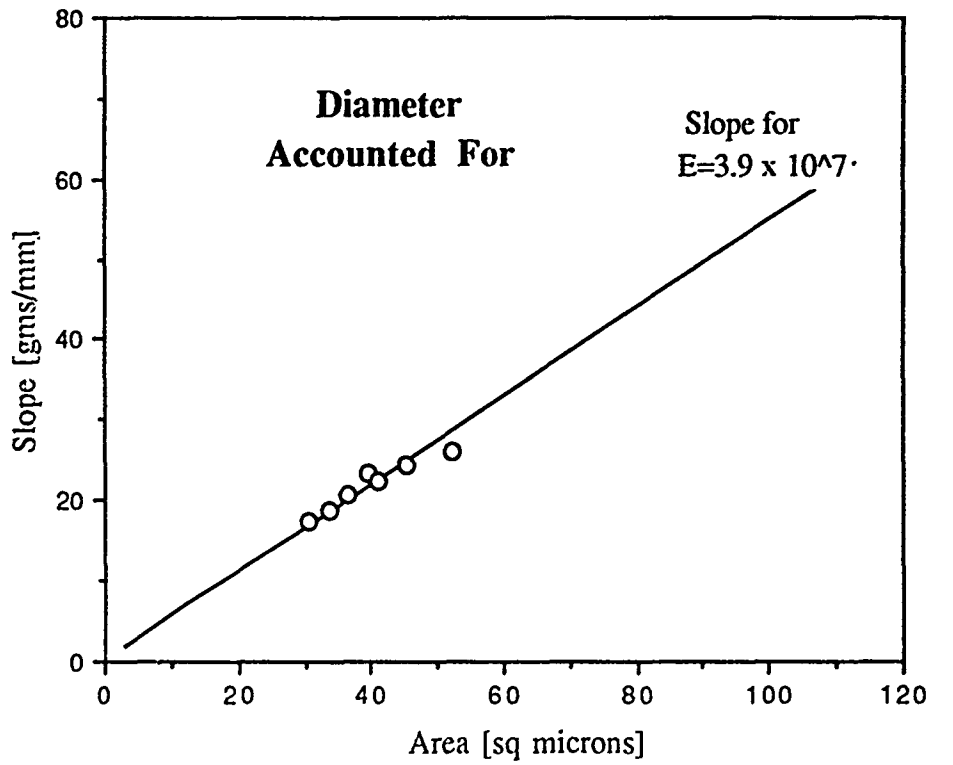

Figure 19. Consistent Modulus When Diameter Accounted For

V. PARAMETRIC INFLUENCE INVESTIGATION

The experimental data presented in Chapter four provide benchmark information for AS4 graphite fibers. The shape parameter is in the vicinity of five, the scale parameter in the vicinity of 18, and data points exist that suggest multi-modality. These observations provide the starting point for an investigation into the influence of fiber statistics on composite reliability, using the Chain-of-Bundles model as refined by Harlow and Phoenix [Ref. 7]. Numerical calculations of composite reliability predictions were made using various shape parameters, with values in the range observed during testing. The results of those calculations are presented following an introduction to the Harlow-Phoenix method of numerical calculation.

A. MODEL BACKGROUND

The Chain-of-Bundles model considers a composite as a chain of m short bundles in series. Each bundle has a characteristic length, δ, generally thought to be on the order of several fiber diameters. The number of bundles, m, varies with the size of the structure being modeled, ranging from as small as 10^2 for a laboratory specimen to values of the order 10^7 for an A6 wing. Each bundle has n parallel fibers embedded in matrix. The fiber strengths are taken as independent and identically distributed (i.i.d.) random variables. The fiber strength CDF, F(x), must be determined from fiber testing.

Within each bundle failed fibers carry no load, while non-failed fibers share the entire applied load. The load per fiber for every possible configuration of failed and non-failed fibers is determined by using the local load sharing (LLS)

rule, as discussed in section II.C.1. Bundle strengths for n fibers, defined to be $G_n(x)$, are also assumed to be independent and identically distributed random variables. Because the bundles are in series, the weakest link formula applies for composites modeled by a chain of bundles. Therefore, $H_{m,n}(x)$, the CDF for composite tensile strength of m bundles, is

$$H_{m,n}(x) = 1-[1-G_n(x)]^m \tag{5.1}$$

It is clear that once the bundle distribution, $G_n(x)$, is known, composite reliability calculation is straightforward.

Recall that current understanding of composite fracture is by sequential fiber failure. Harlow and Phoenix provided the mathematical formulations that account for all possible combinations and permutations of failed/non-failed fiber configurations during sequential failure. The steps required to calculate $G_n(x)$ were listed in section II.C.2, and are repeated here for convenience:

- All possible *states* of failed and surviving fibers are accounted for.
- Load factors for each state are generated according to the LLS.
- All possible failure *sequences* are generated.
- The probability of each sequence occurring is generated. These probabilities depend on single fiber statistics.
- The probabilities for all sequences are summed to obtain overall probability of composite structure failure for a given load.
- The process is repeated for various loads over the range of interest.

B. THREE FIBER EXAMPLE

An example of bundle strength determination for a three-fiber-in-matrix composite is presented here to explain the mathematical formulation of chain-of-

bundles calculations. Note that calculations performed using either the LLS or ELS rule yield identical results for three or fewer fibers, but different results for any number greater than three. A three fiber example is chosen here because it is the smallest size that illustrates the influence of fiber statistics on sequential failure using the LLS rule, while the physical failure process is not obscured by mathematical complexity.

1. Uni-modal Case

Consider first the case of fiber strengths that are described by single shape and scale parameters over all ranges (i.e. uni-modal distribution). The fibers are arranged in a circular array as shown in figure 20. The load factor for a surviving fiber using the LLS rule is K_r where $K_r = 1+r/2$. Figure 20 also lists all possible configurations of failed and surviving fibers. The entries within parenthesis are the associated load factors for fibers one, two and three, respectively.

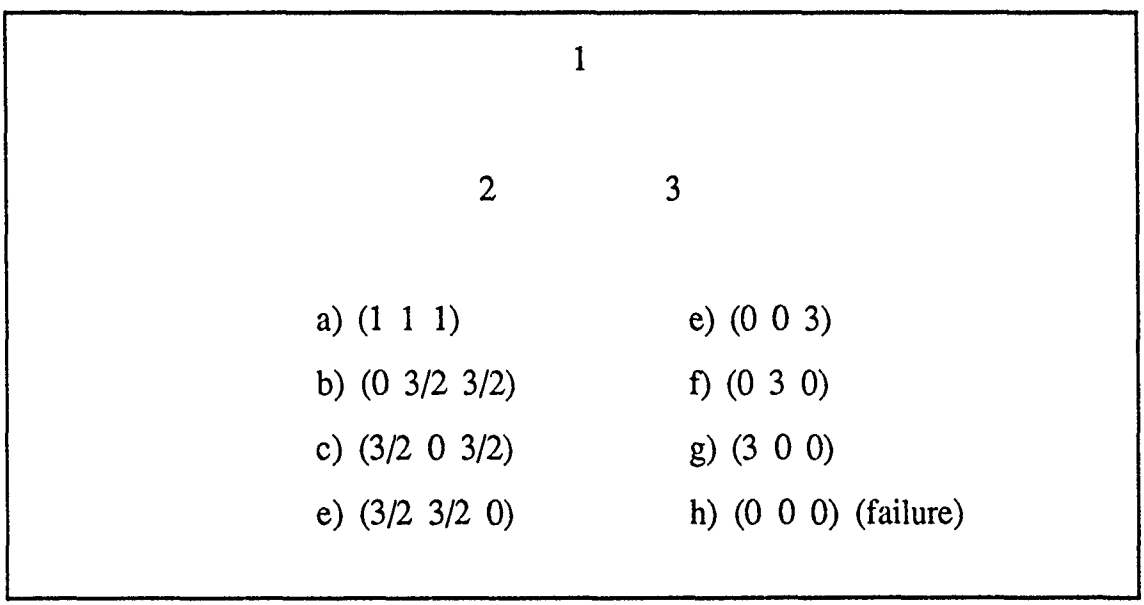

Figure 20. Configurations of Failed/Non-failed Fibers With Load Factors

With an external load of p (per fiber) applied to the bundle, failure will occur if fiber strengths permit a progression through any possible sequence of states. For example, with X_1, X_2, and X_3 the randomly distributed strengths of fibers 1,2, and 3 respectively, if

$$X_1 \leq p,\ p < X_2 \leq 3p/2,\ 3p/2 < X_3 \leq 3p$$

failure sequence [a-b-e-h] would occur, whereas if

$$X_1 \leq p,\ X_2 \leq p,\ p < X_3 \leq 3p$$

then failure sequence [a-e-h] would occur. Note that if any one inequality does not hold, composite failure does not occur. As stated, the probability of composite *bundle* failure requires computing and summing the probabilities of all possible sequences, which are listed in figure 21.

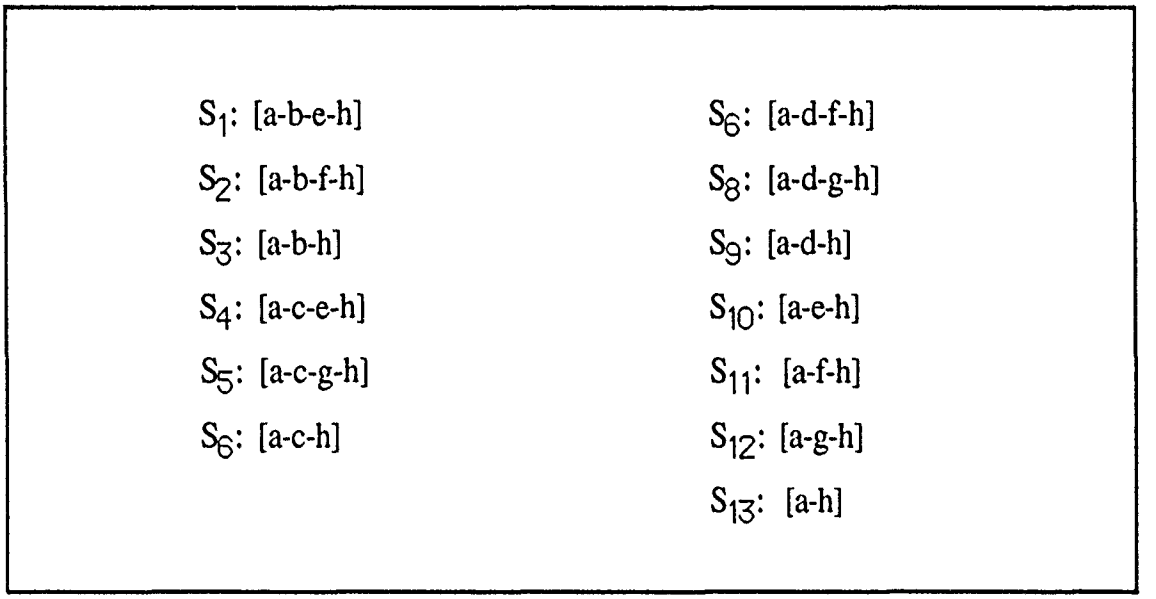

Figure 21. Possible Failure Sequences for a Three Fiber Composite

Determining the probability associated with any sequence can best be illustrated with a sample calculation. The probability that sequence S_1 will occur would be computed as follows:

Let: E_1 = event that $X_1 \leq p$

E_2 = event that $p < X_2 \leq 3p/2$

E_3 = event that $3p/2 < X_3 \leq 3p$

$P\{E_i\}$ = probability that event i occurs

$P\{S_1\}$ = probability that sequence S_1 occurs

Then: $S_1 = E_1 \cap E_2 \cap E_3$

$$P\{S_1\} = P\{E_1 \cap E_2 \cap E_3\} = P\{E_1\}\, P\{E_2\}\, P\{E_3\} \quad \text{(because i.i.d.)}$$

Where: $P\{E_1\} = P\{X_1 \leq p\} = F(p) = 1\text{-}\exp\{-(p/\beta)^{\wedge}\alpha\}$

$$P\{E_2\} = P\{p < X_2 \leq 3p/2\} = [F(3p/2) - F(p)]$$

$$= [1\text{-}\exp\{-(3p/2/\beta)^{\wedge}\alpha\}] - [1\text{-}\exp\{-(p/\beta)^{\wedge}\alpha\}]$$

$$P\{E_3\} = P\{p/2 < X_3 \leq 3p\} = [F(3p) - F(3p/2)]$$

$$= [1\text{-}\exp\{-(3p/\beta)^{\wedge}\alpha\}] - [1\text{-}\exp\{-(3p/2/\beta)^{\wedge}\alpha\}]$$

Obviously the probabilities associated with each event are the probabilities that the given fiber falls in the proper range for sequence S_1 to occur. The overall probability for sequence S_1 is:

$$P\{S_1\} = F(p)\,[F(3p/2) - F(p)]\,[F(3p) - F(3p/2)]. \qquad (5.2)$$

Similarly, the probability of sequence S_{10} [a-e-h] is:

$$P\{S_{13}\} = F(p)\,F(p)\,[F(3p) - F(3p/2)] = [F(p)]^2\,[F(3p) - F(3p/2)]$$

The probabilities of sequences S_1 through S_{13} must all be calculated and summed to determine the probability of bundle failure, $G_3(p)$, under applied load p per fiber. The *distribution of bundle strengths*, $G_3(x)$, is found by repeating the above calculations for different values of x over the range of interest. From this distribution, composite strength may easily be calculated from equation (5.1).

Figure 22 shows the dependence of sequence probability calculations on fiber statistics for the uni-modal case. Obviously if α or β are changed, the failure probabilities for p, 3p/2, and 3p will also change, altering sequence probabilities and bundle strengths as well. Harlow and Phoenix performed numerical calculations for composites with up to nine fibers, for a range of different shape parameters, assuming uni-modal fiber statistics. The reader is referred to Ref. 7 for further details.

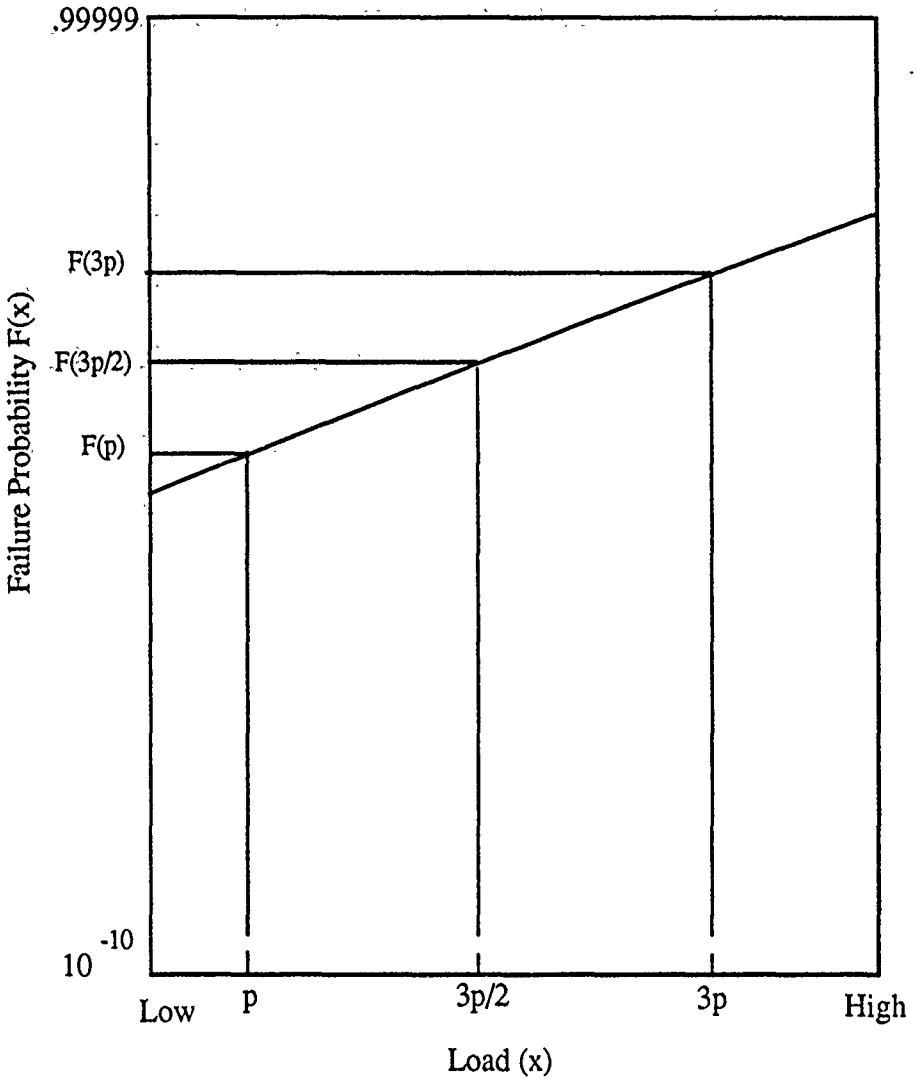

Figure 22. Uni-modal Distribution

2. Tri-modal Case

Figure 23 shows one possible tri-modal distribution of fiber strengths. The graph is divided into three regions: low (L), middle (M), and high (H), with associated shape and scale parameters for each region.

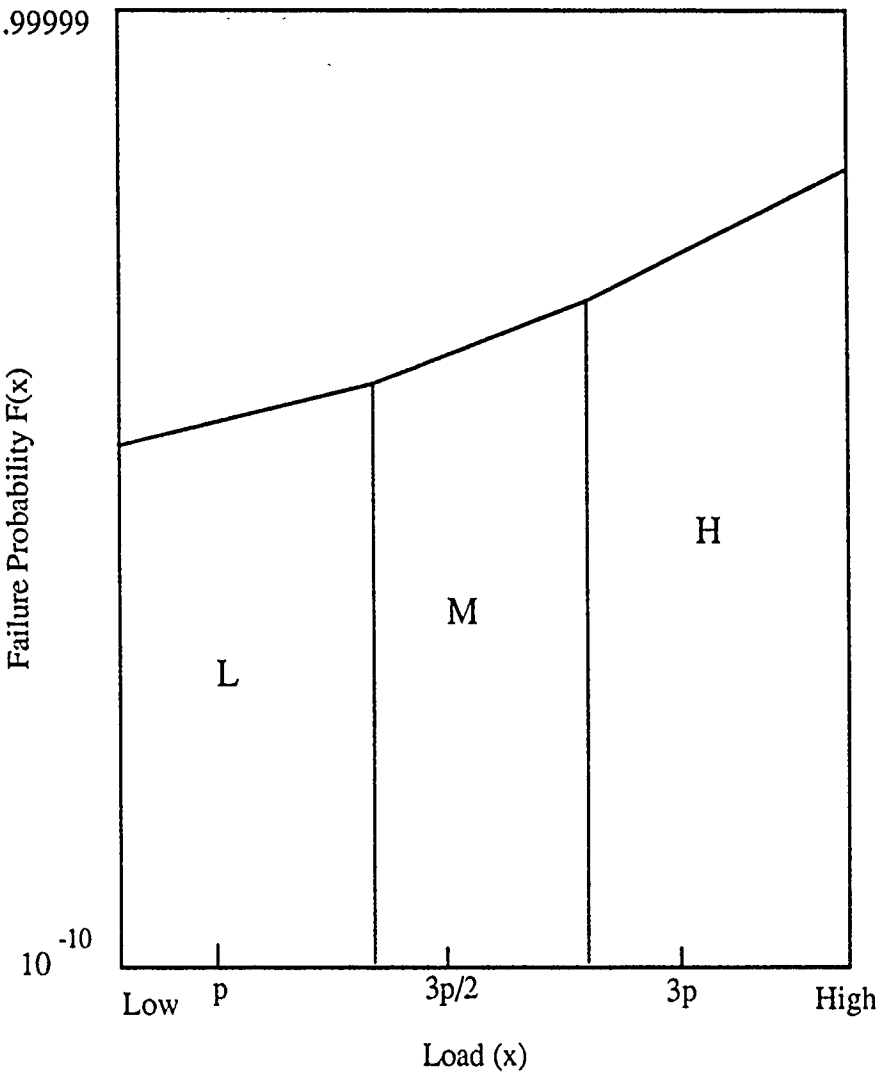

Figure 23. Tri-modal Distribution

The mathematical formulations are the same as for the uni-modal case except that now F(p) is replaced by $F_L(p)$, $F_M(p)$, or $F_H(p)$ for the appropriate region. Using the same notation as for the uni-modal case, the probability of sequence S_1 is now calculated by:

$$P\{X_1 \le p\} = F_L(p) = 1\text{-}\exp\{-(p/\beta_L)^{\alpha_L}\}$$

$$P\{p < X_2 \le 3p/2\} = [F_M(3p/2) - F_L(p)]$$

$$= [1\text{-}\exp\{-(3p/2/\beta_M)^{\alpha_M}\}] - [1\text{-}\exp\{-(p/\beta_L)^{\alpha_L}\}]$$

$$P\{p/2 < X_3 \le 3p\} = [F_H(3p) - F_M(3p/2)]$$

$$= [1\text{-}\exp\{-(3p/\beta_H)^{\alpha_H}\}] - [1\text{-}\exp\{-(3p/2/\beta_M)^{\alpha_M}\}]$$

$$P\{S_1\} = F_L(p)\,[F_M(3p/2) - F_L(p)]\,[F_H(3p) - F_M(3p/2)] \qquad (5.3)$$

The effect of the using a uni-modal versus tri-modal assumption can be seen by comparing equations (5.2) and (5.3). The effect is more easily seen graphically. Figure 24 shows the differences between uni-modal and multi-modal probabilities for the current example.

Table IV, reading left to right, compares the factors used in equations (5.2) and (5.3). Clearly the probability associated with sequence S_1 (and all others) is different for uni-modal vice this multi-modal case, but whether larger or smaller cannot be determined without numerical calculations since the individual factors do

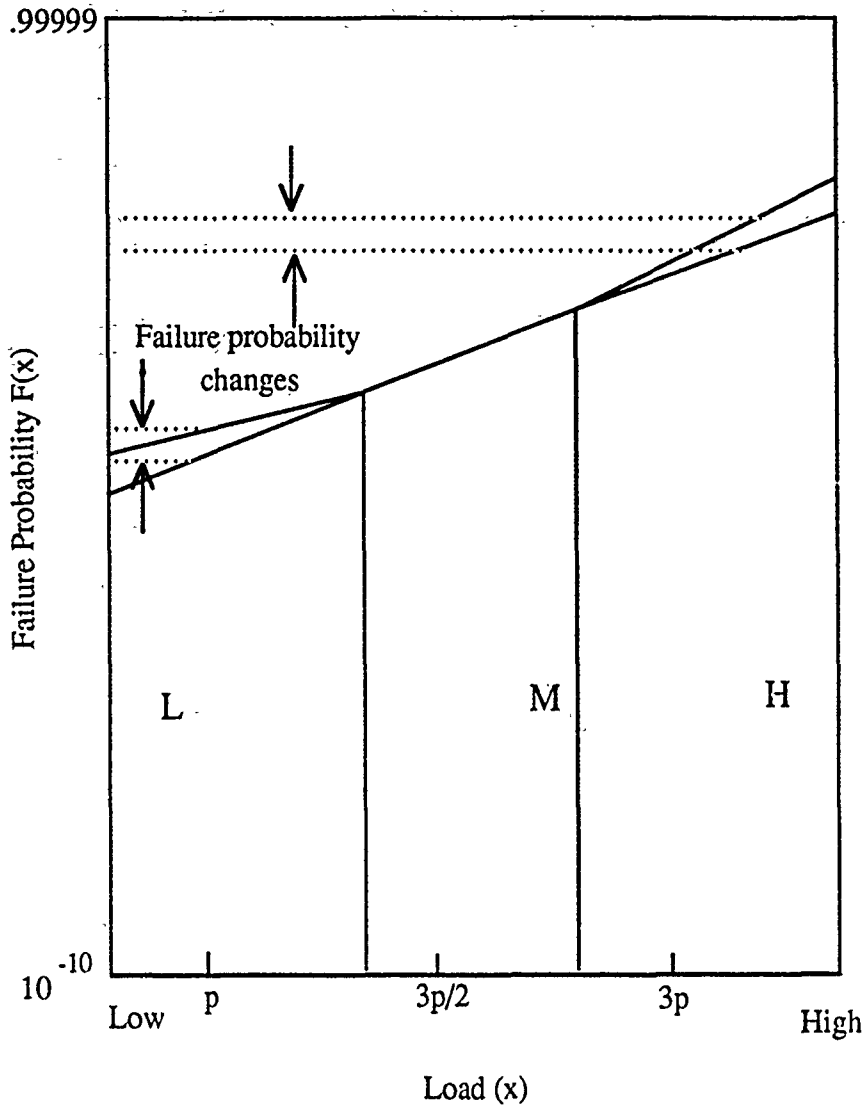

Figure 24. Effect of Tri-modal Distribution

TABLE VI. Tri-modal Versus Uni-modal Factors

	Tri-modal	Relationship	Uni-modal
fiber 1	$F_L(p)$	greater than	F(p)
fiber 2	$F_M(3p/2) - F_L(p)$]	less than	[F(3p/2) -F(p)]
fiber 3	$[F_H(3p) - F_M(3p/2)]$	greater than	[F(3p) -F(3p/2)]

not all change in the same direction. Therefore the effect of multi-modal fiber statistics on three-fiber bundle strength, $G_3(p)$, is also unknown.

This observation can be generalized to bundle strength, $G_n(x)$, for any n, with the result that composite reliability, $H_{m,n}(x) = 1-[1-G_n(x)]^m$, is also affected by fiber modality in an uncertain manner. Numerical calculations must therefore be performed to quantitatively determine the fiber upper and lower tail effects on composite reliability.

C. NUMERICAL CALCULATIONS

Harlow and Phoenix [Ref. 7] determined that under the LLS rule, large composites act in a weak link manner. $W_n(x)$ is a weakest link scaling of the composite *back to single fiber size*, through the equation

$$H_{m,n}(x) = 1-[1-G_n(x)]^{mn}$$

where $$W_n(x) = 1-[1-G_n(x)]^{1/n}$$

Figure 25 shows the typical relationship between F(x) and $W_n(x)$ for several values of n. (It is convenient to use the dimensionless load, x/β, as the random variable for composite reliability plots. This has been done in figure 25 and will be continued throughout this chapter.) Note that as n increases, $W_n(x)$ appears to rapidly converge to a single curve. From figure 25, we see that once $W_n(x)$ is determined, composite reliability may be read directly from the graph for the load and size of interest. Numerical calculations of $W_n(x)$ in this investigation were performed for n=6, with various combination of input parameters for the three regions of the tri-modal model.

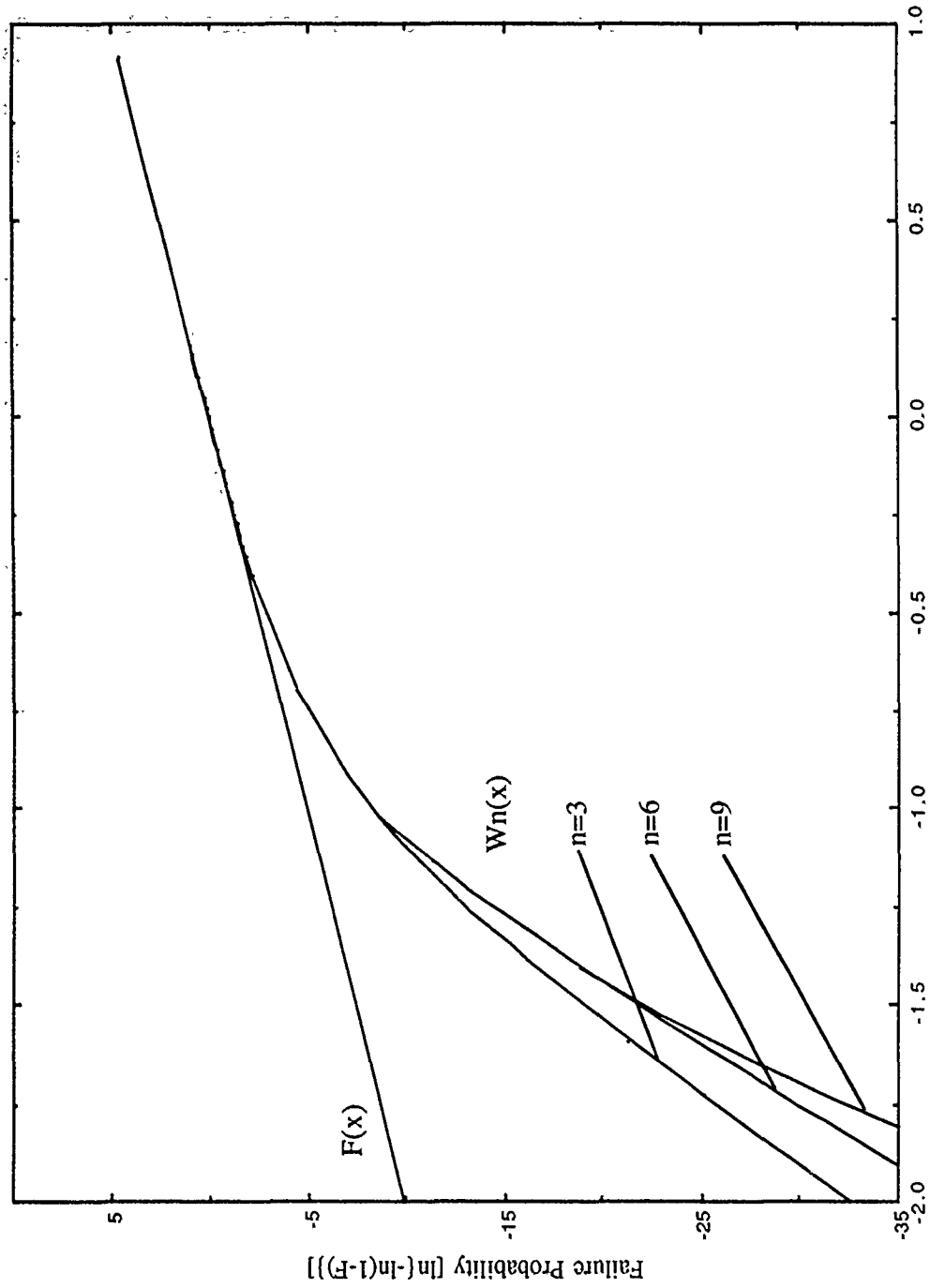

Figure 25. F(x) and Wn(x)

1. Physical Considerations

General consensus among statisticians is that more than three parameters to describe any data set is redundant. While it may be true that three parameters will fit a curve with sufficient accuracy to any set of experimental data, the intent here is not to generate a curve, but rather to accurately model the physics of the fiber strength distribution. Considerations such as damage to fibers during the stranding process (weak lower tail), proof testing (strong lower tail), or hybrid composites (weak lower tail and strong upper tail) all suggest that tri-modal characteristics (requiring five parameters) should be explored. For this investigation, reasonable values for lower, middle and upper shape parameters were determined from experimental data, as were the transition points between the three regions (see figure 26).

2. Answers Sought

For all numerical calculations, load was non-dimensionalized by the scale parameter, β. The lower-to-middle transition point was $x/\beta=0.7$, the middle region scale parameter was 1.0, and the middle-to-upper transition point was $x/\beta=1.2$. Nine calculations were performed to include all combinations of

$$\alpha_L = 3, 5, \text{or } 7$$
$$\alpha_M = 5$$
$$\alpha_H = 3, 5, \text{or } 7.$$

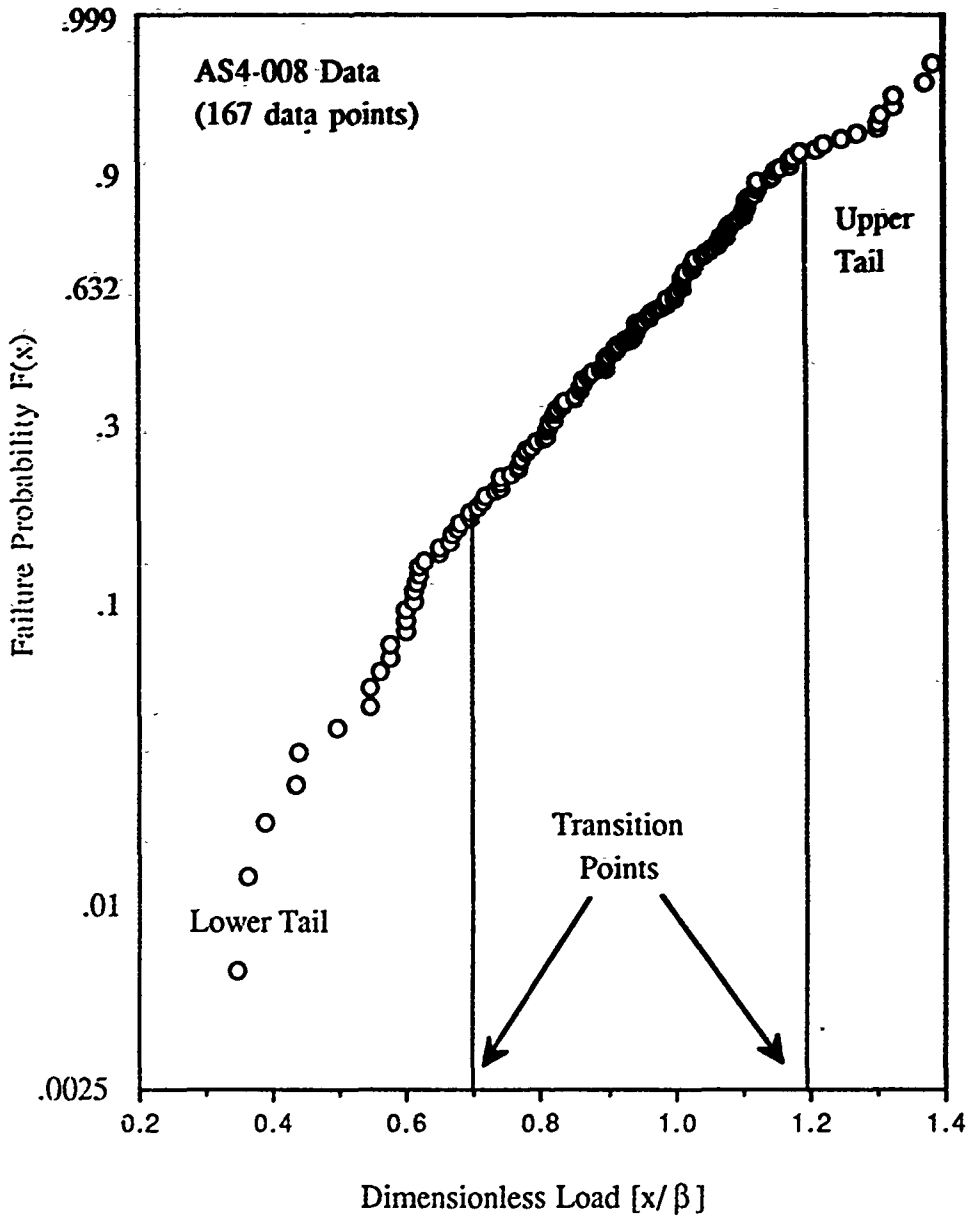

Figure 26. Multi-Modal Transition Points From Experimental Data

The answers to four general questions were sought with respect to the influence of fiber extreme tails on the composite performance:

- **Q1: How much does the lower tail affect composite reliability by itself?**
- **Q2: How much does the upper tail affect composite reliability by itself?**
- **Q3: Can a strong upper tail compensate for a weak lower tail ?**
- **Q4: Does a weak upper tail diminish the effect of a strong lower tail?**

D. PARAMETRIC INFLUENCE

1. Lower Tail Effects

Fiber lower tail effects on composite reliability were investigated by numerical calculations with respective fiber shape parameters $\alpha_M = \alpha_H = 5$, and $\alpha_L = 3$(weak tail) or $\alpha_L = 7$(strong tail).

a. Weak Lower Tail

Weak lower tail fiber statistics have a strong adverse effect on composite reliability , as observable in figure 27. For example, for a non-dimensionalized load of 0.18, composite reliability decreases from 10^{-12} to 10^{-9},(three orders of magnitude!) when the lower tail shape parameter is decreased from five to three.

b. Strong Lower Tail

Strong lower tail fiber statistics have a large beneficial effect on composite reliability, as seen in figure 28. For the same non-dimensionalized load

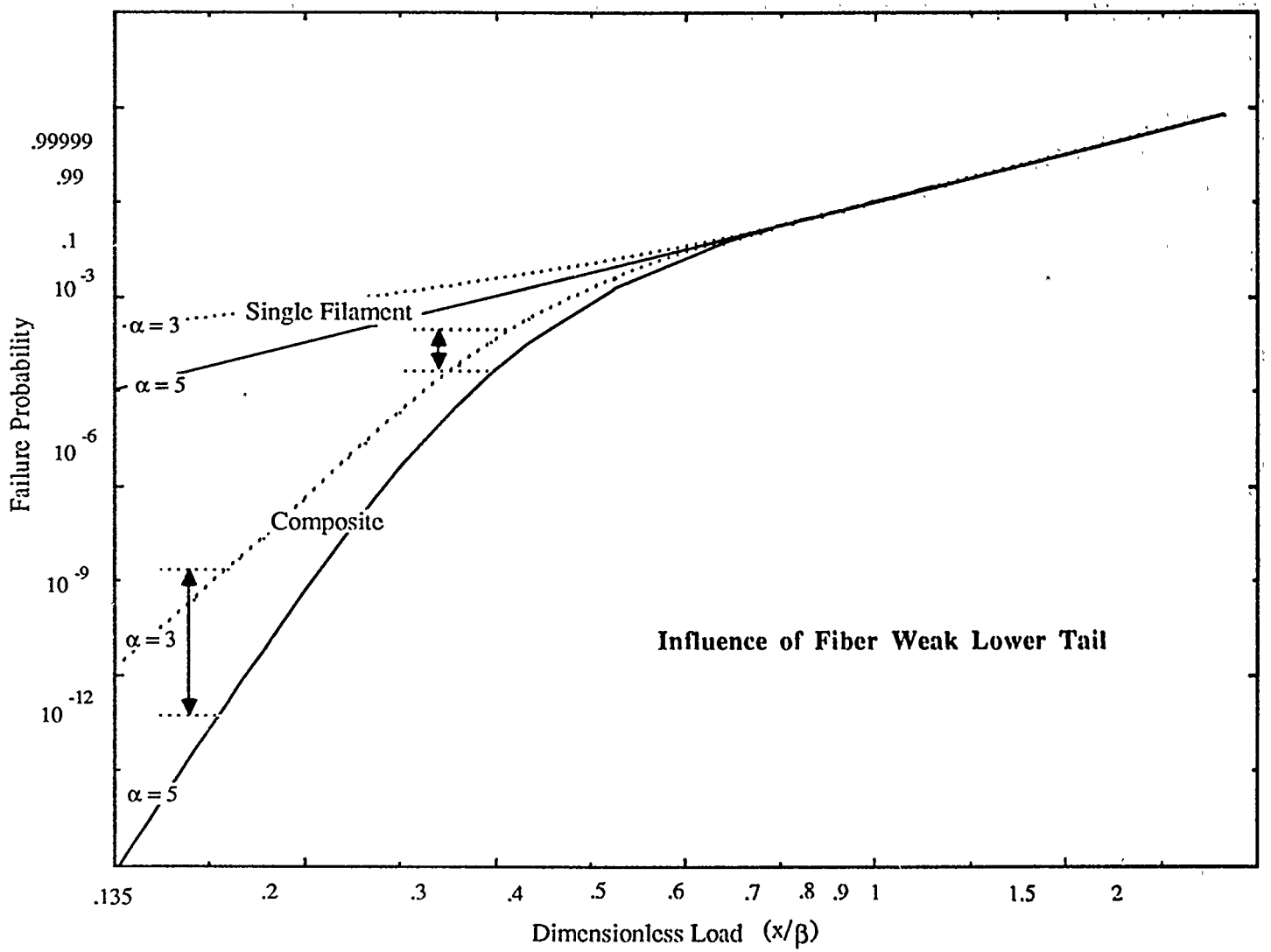

Figure 27. Influence of Fiber Weak Lower Tail on Composite Reliability

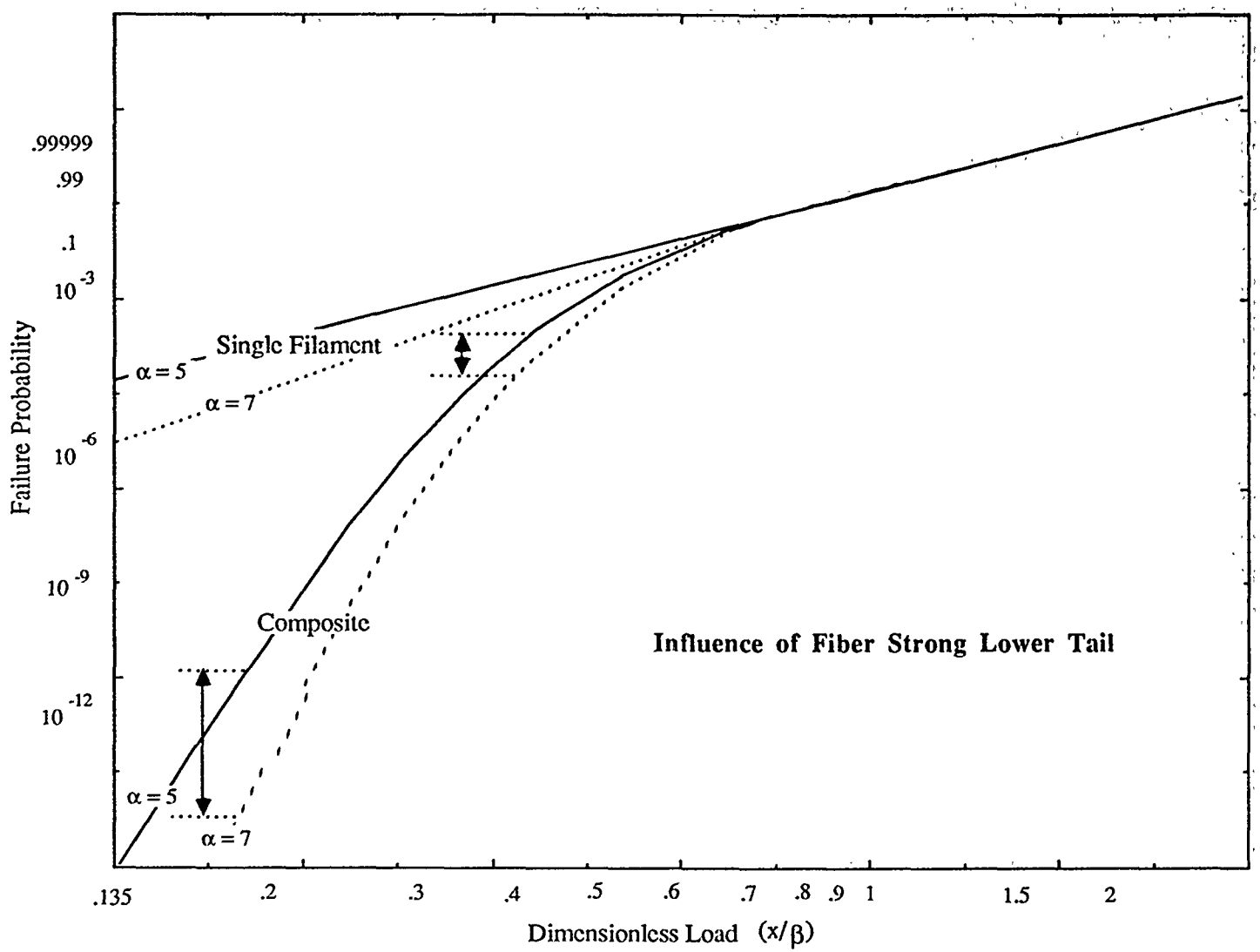

Figure 28. Influence of Fiber Strong Lower Tail on Composite Reliability

of 0.18, composite reliability increases from 10^{-12} to 10^{-15} when the lower shape parameter is increased from five to seven.

c. Implications

The answer to Q1 is clear: the fiber lower tail has a very strong influence on composite reliability. This result has implications for acceptance testing and design. The dramatic decrease in composite reliability caused by a weak lower tail indicates that sufficient fiber testing must be conducted to determine lower tail characteristics before composite construction begins. Likewise, while proof testing is known to benefit reliability, the strong-lower-tail results of this test serves to *quantify* the gains that may be expected.

2. Upper Tail Effects

a. Weak or Strong Upper Tail

Upper tail effects on composite reliability were investigated by numerical calculations with $\alpha_L = \alpha_M = 5$, and α_H=3(weak tail) or α_H= 7(strong tail). Upper tail variations were observed to have no influence on composite reliability within the range of interest, as evident in figure 29.

b. Implications

The answer to Q2 is also clear: the upper tail by itself has no influence on composite reliability in the range of interest. The absence of upper tail influence, particularly the lack of reliability improvement with a strong upper tail, has important implications for Navy Specifications and acceptance testing. Manufacturing processes may be optimized to strengthen the upper tail of the fibers relatively, without a commensurate improvement in lower tail characteristics. An apparent fiber improvement would be manifested by an increased mean strength (especially if a uni-modal assumption is made), but the

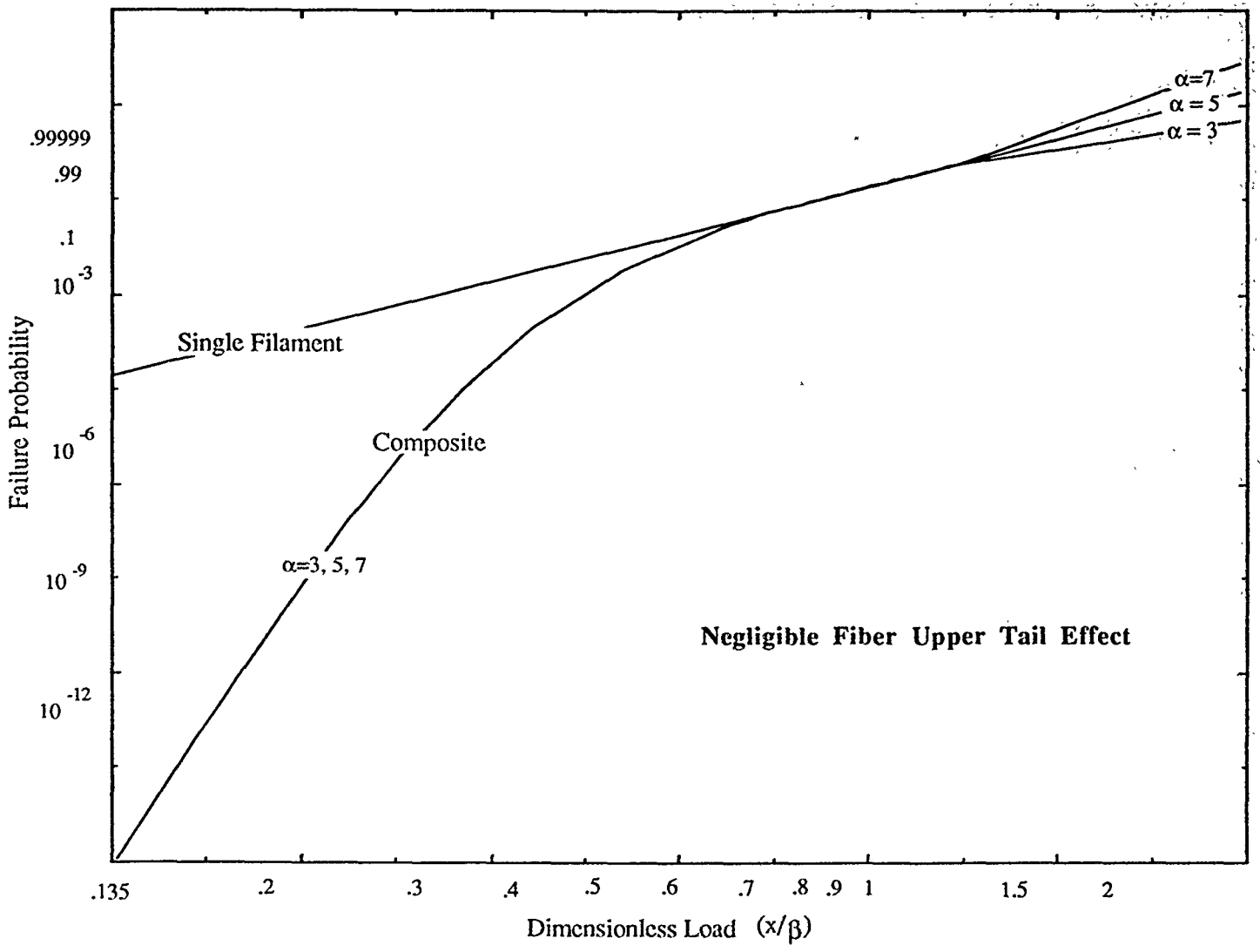

Figure 29. Influence of Fiber Upper Tails on Composite Reliability

improvement will contribute practically nothing toward increased composite reliability.

3. Combined Effects

The answers to questions Q3 and Q4 were determined by numerical calculations with all combinations of weak and strong lower tails with weak and strong upper tails. No combination was found in which the upper tail had any influence (neither strengthening nor weakening) on composite reliability.

a. Implications

These results suggest that hybrid composites with the same modulus (composites with a mix of strong and weak fibers, used as a cost saving measure) should not be used in applications where high reliability is required since the weak fibers will greatly reduce composite reliability while the strong fibers will do little or nothing to improve it. This does not argue against all hybrid composites. On the other contrary, hybrid composites made of fibers with different moduli can be used to effectively *shift* the probability of failure among the low, medium or high regions, thereby resulting in significant benefits to the composite reliability.

E. APPLICATIONS

As discussed in section C of this chapter, $W_n(x)$ is a weakest link scaling of the composite back to single fiber size. Therefore, the ordinate on Weibull probability paper can be used to compare size effects using the $W_n(x)$ curve. Moving down on the vertical scale is equivalent to either increased size or increased reliability for a composite structure. Figure 30 is useful in illustrating the implications of size effects. Given that single fiber testing must be sufficient to reveal lower tail behavior in the region of interest, figure 30 shows that for small structures (region

B), as few as 100 fiber tests ($1/10^{-2}$) may be sufficient, whereas for large structures such as a submarine hull (region A),as many as 10,000 fiber tests ($1/10^{-4}$) may be still be insufficient.

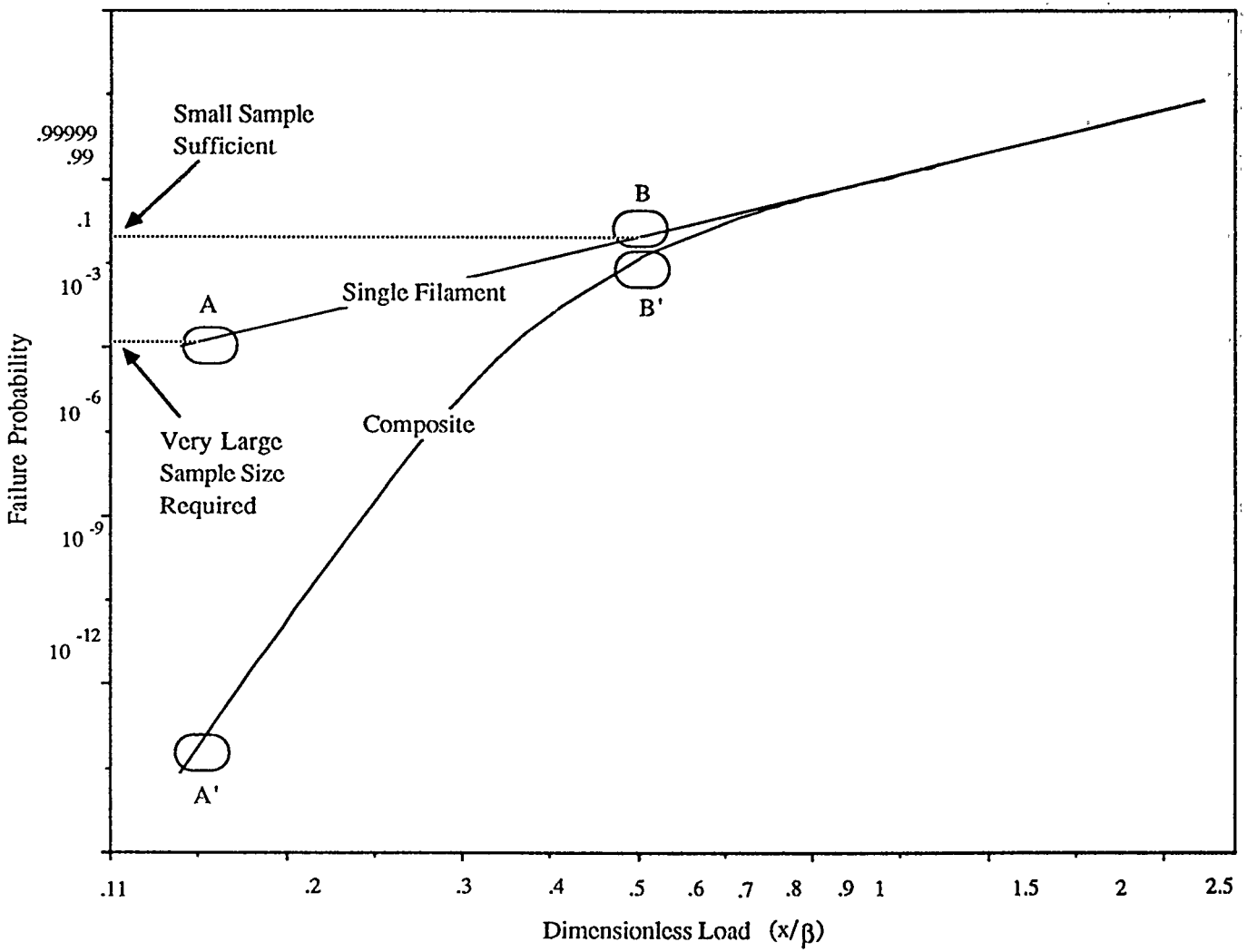

Figure 30. Size Effect and Implications for Single Fiber Testing

VI. CONCLUSIONS

The primary goal of this research effort was achieved in that uncolored fiber statistics were acquired from carefully refined, executed and documented experimental procedures. The procedures themselves serve as guide for future testing, and development of more expedient alternatives to single fiber testing. The data serve as a benchmark to evaluate different probability models which relate fiber statistics to composite reliability.

Sufficient data were acquired to allow meaningful interpretations which have been discussed in chapters four and five. The most important ones are summarized here:

- Single fiber statistics for AS4 graphite fibers do in fact exhibit Weibull weakest link behavior as predicted by the analytical model.
- Observed lower tail behavior for both sets of test data suggest that a multi-modal Weibull description may be appropriate.
- The data indicated a difference between fiber strengths from the two different spools, and this difference was consistent with observations made during composite testing of the same two spools.
- Fiber failure load and fiber diameter appear to be independent random variables.
- Results regarding the variability of stress vice load as the random variable were inclusive.
- Composite reliability (especially for large structures) is extremely sensitive to fiber lower tail behavior, but insensitive to upper tail behavior in the region of interest.

Given these results and interpretations, it is concluded that uncolored fiber statistics *can* be acquired if sufficient care is taken. Furthermore, uncolored fiber statistics are crucial because of the lower tail's strong influence coupled with the

indications that AS4 graphite fibers have an intrinsically weak lower tail. The procedures used in this investigation should be continually refined for research applications. At the same time, efforts should be made to adapt them for Navy acceptance testing and industrial quality control procedures, and identification of the most effective direction for new fiber development.

APPENDIX A. FIBER SAMPLE PREPARATION

The importance of fiber statistics *uncolored* by experimental implementation has been repeatedly demonstrated throughout this investigation. The single most important element in achieving uncolored fiber statistics is the preparation of samples to be tested. Therefore, this appendix is designed to be stand-alone documentation of the procedures used in this research, which may be used as a guide for follow-on testing. An overview of the process will be presented, followed by a step by step consideration of the care required throughout the sample preparation sequence.

A. OVERVIEW

1. Sources of Bias

Two significant sources of bias to the data were identified:

•Fiber samples not selected at random.

•Fibers damaged prior to test.

Non-random selection of fiber samples is most likely to occur when the selection process results in the weak fibers being broken prior to test. This effectively eliminates the lower tail and causes the data to exhibit less variability than the "true" underlying population's intrinsic variability.

Fiber damage through handling prior to test can have several different effects. If all samples are damaged approximately the same amount, the effect is to shift the entire distribution to the left (i.e. reduced scale parameter,but unchanged shape), leading to the belief that the fibers are weaker than they actually are. While this would lead to errors in the conservative direction, it would lead to over-design of structures with unnecessary additional expense and weight. On the other hand, if

some fibers are damaged more than others the effect is to increase the variability (i.e. reduced shape parameter) of the observed data, with an uncertain effect on the scale parameter. This is considered to be the more likely case.

2. Sample Preparation Sequence

Graphite fibers came from the manufacturer as one continuous strand of essentially untwisted fibers (of order 10^5 fibers per strand) wrapped around a spool. Short segments were cut from the spool, from which individual fiber samples were extracted and mounted on 3" x 5/8" cardboard strips. No more than ten samples were taken from any given segment to ensure that a representative set of fiber samples was obtained from different locations along the strand. The bundle segments were prepared for single-fiber extraction by taping one end of the segment to a glass plate and fanning the fibers out at the other end (figure A1).

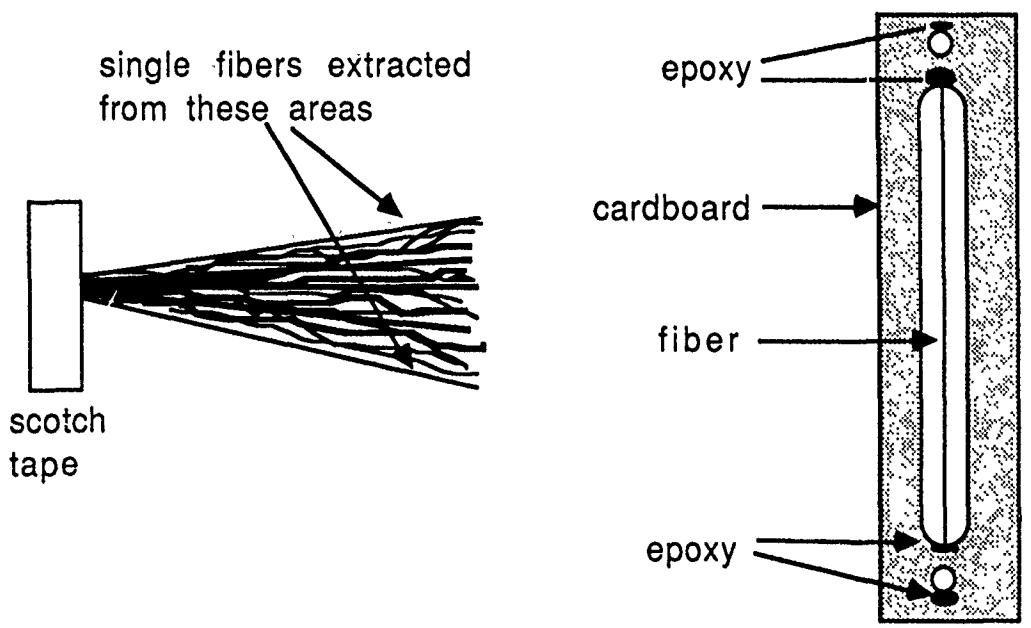

Figure A1. Fiber Bundle Prepared For Single Fiber Extraction

After mounting, the fiber was secured to the cardboard with epoxy. Epoxy was also placed around the holes in the cardboard to strengthen it in the area where load was transmitted during tensile strength testing.

The potential sources of fiber damage during handling fell into four broad categories:

- •Surface friction - caused when a fiber rubs against its neighbors while being extracted from the original strand.
- •Bending stress - caused when the fiber is bent during the fiber mounting process, causing tensile stress on one side of the fiber and compressive stress on the other.
- •Twisting - caused when one end of the fiber is "rolled" while the other end is held fixed during extraction from the original strand.
- •Notching - caused when the fiber is struck by a sharp object that could put a notch in the fiber surface.

The procedures used to avoid these sources of damage are detailed in the following paragraphs.

B. SAMPLE PREPARATION CONCERNS

1. Segment Cut From Spooled Strand

There were two major concerns at this stage. The first was to insure that while handling the spool, neither it nor the segment being cut was bumped by anything hard that could cause notch damage. The other concern was the length of the segment cut. It had to be long enough to allow handling the *ends* of the segment while leaving the center, which became the 50 mm test section, completely untouched. A segment too long, however, was prone to entanglement of the individual fibers which increased the risk of skin friction damage or bending

stresses during fiber extraction. Five to six inches was determined to be a good compromise length.

2. Fibers Fanned Out

During this stage there were three major concerns. Surface friction damage was most likely to occur here as fibers rubbed against each other. Surface friction was minimized by bathing the entire strand in alcohol during the fanning out process.

The second concern was twisting of the fiber that was targeted for extraction. While moving a single fiber clear of the bundle, care had to be taken not to roll the free end of the fiber with a finger. To avoid this, the free end of the fiber was picked up with a small piece of scotch tape and gently moved to the desired location.

The third concern was bending stress. Bending stress calculations show that if a fiber is bent around a radius of one inch, the surface will experience a strain of approximately .0003, which is several orders of magnitude below the typical strain at failure and not considered capable of causing damage. Therefore, a minimum radius of one inch for fibers during handling was used for this investigation. An insidious problem encountered during the fanning out process was that often a large percentage of the fibers in the strand would be bent momentarily to a smaller radius, and then revert back to a near straight condition, such that it was impossible to tell whether or not a particular fiber had been damaged by bending. The solution to this problem was to extract fibers only from the edges of the bundle, as shown in figure A1, and only those fibers whose history was known for certain.

3. Fibers Extracted From Bundle

The major concern here was to not inadvertently break weak fibers in the extraction process. Extracting the fibers radially was almost sure to produce this result. The solution was to choose only fibers near the edge of the bundle and to carefully lift the fiber's free end, with a minimum of tensile force, to place it directly over the cardboard strip for mounting. Extreme care had to be taken at this stage to not bump the fiber against the edge of the cardboard strip, or surface notch damage could have occurred.

4. Mounting Fibers

The major concern for fiber mounting was to eliminate sources of error to strain data. When a tensile load was applied to the fiber through the cardboard strip whose sides had been burned away, if the fiber slipped at its attach point, the slippage would have been recorded as sample deformation. Likewise, if the holes in the cardboard were elongated by the test equipment, that elongation would also have been recorded as sample deformation. The solution was to use a strong epoxy bonding agent to attach the fiber to the cardboard, and the epoxy was also applied around the holes to strengthen them against elongation. After epoxy application, the cardboard strips were heated to approximately 150 degrees Fahrenheit for several minutes to promote epoxy absorption by the cardboard.

5. Fiber Storage Prior to Test

At this point the sample cardboard strips were longer be handled with fingers, but with tweezers. They were stored in such a way that the fibers themselves were not in contact with anything, and the risk of inadvertent bumping was minimized. Fibers that were inadvertently bumped by a hard object were discarded immediately, and not tested "to see if any damage had occurred."

APPENDIX B. FIBER DIAMETER MEASUREMENT

Fiber diameter measurements were made with the NPS Integrated test System (NPSITS). Based on classic Fraunhofer diffraction theory, the NPSITS calculates fiber diameter based on the interference nodes, or minima, of a diffraction pattern produced when the fiber is illuminated by a laser beam. Previous thesis research by Bennett [Ref. 14] demonstrated that the minimums could be located using a photo conductive cell (MicronEye™), which yielded reasonable results. Thesis research by Storch [Ref. 15] examined the nature of the diffraction pattern itself and the effects of varying MicronEye™ exposure time. Further work by Kunkel [Ref. 10] refined the laser-fiber-MicronEye™ geometry used, automated the data acquisition process, and automated the calculation of diameter based on laser diffraction theory.

This investigation, using the same instrumentation with slightly modified procedures, was able to achieve repeatability in diameter measurements estimated to be well within 0.3%.

A. PROCEDURE

Each cardboard mounted fiber was placed in the test stand with the fiber centered in the laser beam (figure B1). The operator then manually positioned each MicronEye™ until the diffraction pattern node was centered on the MicronEye™ image. This fixed the X distance (figure B1) which was then used to calculate fiber diameter using the Macintosh™ application CALIPER [Ref. 10].

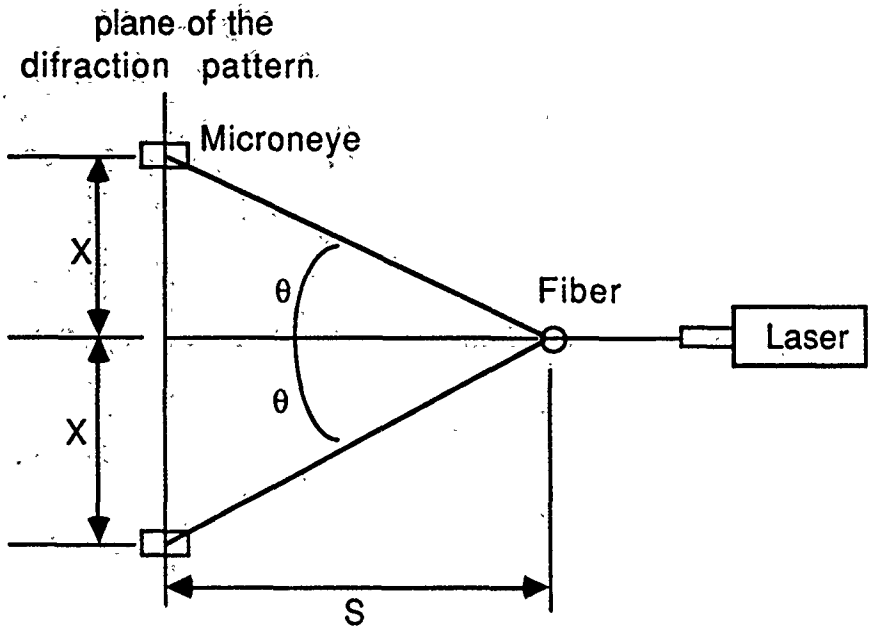

Figure B1. System Geometry

Initially the distance from fiber to MicronEye™ plane of diffraction pattern (S distance in Figure B1) was varied until an optimum distance was found (0.84 meters). Once optimized, the S distance remained fixed for the duration of testing. The optimum distance reflected the tradeoff between :

1. Amplified signal to noise ratio as S increased (making centering of the node very imprecise, thus producing a large uncertainty in the X distance).
2. The increased sensitivity to error of scattering angle θ as X distance decreased (i.e. X could be determined more precisely as S decreased, but θ, hence calculated fiber diameter, became extremely sensitive to even small errors in X).

B. TECHNIQUE

Figure B2 shows the geometry of the fiber and MicronEyes™ with respect to the diffraction pattern. Note that the operator manually repositions

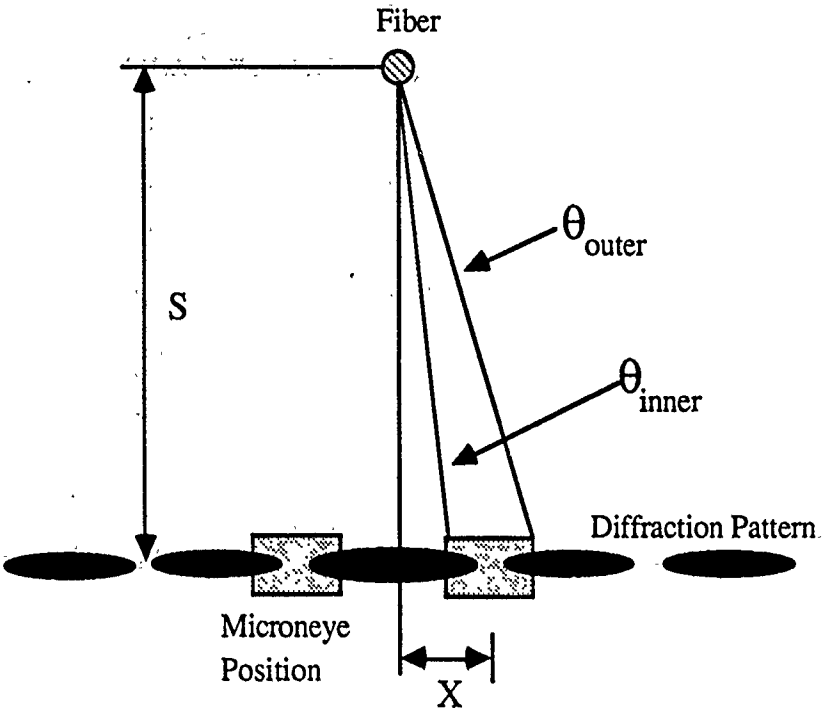

both

Figure B2. MicronEye™ Positioning with Respect To Diffraction Pattern

MicronEyes™ to include the desired area of the diffraction pattern for each new fiber measured. The accuracy of the diameter measurement depends on how accurately the distance between nodes is determined, which in turn depends on how accurately the operator centers each MicronEye™ on its interference node. The solution to Kerker's equation (used to calculate fiber diameters) requires knowledge of intensity ratios for the diffraction pattern, which correspond to the user controlled exposure time for the MicronEye™. (See Ref. 15 for a discussion of Kerker's equation and light intensity ratios.)

Unfortunately, for reasons not understood at this time, there was no one exposure time that worked for all fibers. Therefore, the operator had to iterate exposure times for each new sample until one suitable for that particular fiber was achieved. Significant operator judgement was required at this stage.

Because of the significant amount of operator interaction and judgement required, data repeatability for different operators was tested to demonstrate the validity of the procedure. Ten fibers were measured independently by each operator. The results are compared in Table B1. The largest difference between operators was less than 0.2%. This exceptional repeatability confirms the decision to use a relatively long distance between the fiber and the MicronEye™ plane (S-distance) in order to reduce the sensitivity to errors in MicronEye™ lateral positioning (X-distance).

C. SCANNING ELECTRON MICROSCOPY COMPARISON

Six of the fibers used in the repeatability tests were also measured with a scanning electron microscope (SEM). One of the six could not be measured reliably with the SEM because the fiber edges could not be brought into focus. Measurements for the other five fibers are compared with NPSITS measurements in Table B2.

TABLE B1. Diameter Measurement Repeatability Test

Fiber Sample No.	Operator A	Operator B	Change
1	7.457μm	7.448μm	.12%
2	7.461μm	7.463μm	.03%
3	7.033μm	7.020μm	.18%
4	7.037μm	7.028μm	.13%
5	6.903μm	6.896μm	.10%
6	6.735μm	6.732μm	.04%
7	6.871μm	6.868μm	.04%
8	6.836μm	6.825μm	.16%
9	7.067μm	7.073μm	.08%
10	7.131μm	7.125μm	.08%

TABLE B2. NPSITS and SEM Comparison

Sample	NPSITS	SEM	Change	NPSITS Rank	SEM Rank
5	6.73	7.15	6%	1	1
6	6.90	7.26	5%	2	2
3	7.03	7.71	10%	3	3
1	7.46	8.16	9%	4	4
2	7.46	8.23	10%	4	5

The most important aspect of the data in Table B2 is the agreement in rank between the NPSIT and SEM measurements. Additionally, the two are in fairly

close agreement on an absolute scale (5-10%). Further testing (perhaps 10 more samples) should be conducted to better define the difference between measurements. At that time, the NPSITS may be calibrated through correction factors available in the CALIPER application software. Any number of fiber "standards" may also be measured and stored. This will provide the NPS Advanced Composites Lab with the capability to do in-house calibration any time the system geometry is altered.

APPENDIX C. FIBER TEST DATA

AS4-008 Data
(Operator A)

	Sample	Min Diam	Max Diam	% Change	Avg Diam	P(max)	(In PSI) Stress(max)
1	XA1	7.097	7.174	1.085	7.136	10.263	3.65E+05
2	XA2	6.982	7.147	2.363	7.065	23.442	8.50E+05
3	XA3	7.142	7.432	4.060	7.287	16.186	5.52E+05
4	XA4	6.564	6.605	0.625	6.585	10.973	4.58E+05
5	XA5	7.049	7.098	0.695	7.074	16.031	5.80E+05
6	XA6	7.243	7.355	1.546	7.299	20.310	6.90E+05
7	XB1	7.916	8.130	2.703	8.023	22.964	6.46E+05
8	XB2	6.824	6.853	0.425	6.839	20.956	8.11E+05
9	XB3	7.269	7.387	1.623	7.328	11.485	3.87E+05
10	XB4	7.235	7.281	0.636	7.258	16.487	5.66E+05
11	XB5	7.595	7.601	0.079	7.598	21.906	6.87E+05
12	XB6	6.373	6.561	2.950	6.467	16.390	7.09E+05
13	XB7	6.809	6.950	2.071	6.880	11.901	4.55E+05
14	XC1	6.578	6.625	0.715	6.602	18.602	7.72E+05
15	XC2	7.374	7.399	0.339	7.387	20.078	6.66E+05
16	XC3	7.048	7.200	2.157	7.124	18.553	6.61E+05
17	XC4	7.169	7.218	0.683	7.194	19.579	6.85E+05
18	XC6	6.980	7.306	4.670	7.143	13.237	4.69E+05
19	XD1	6.668	6.759	1.365	6.714	20.424	8.20E+05
20	XD3	7.331	7.436	1.432	7.384	15.310	5.08E+05
21	XD4	7.448	7.613	2.215	7.531	11.378	3.63E+05
22	XD5	8.147	8.255	1.326	8.201	21.062	5.67E+05
23	XD6	7.111	7.217	1.491	7.164	19.882	7.01E+05
24	XD7	6.892	7.048	2.263	6.970	19.502	7.26E+05
25	XE1	7.263	7.295	0.441	7.279	14.286	4.88E+05
26	XE3	7.193	7.263	0.973	7.228	20.341	7.04E+05
27	XE5	7.605	7.670	0.855	7.638	19.983	6.20E+05
28	XE6	7.227	7.283	0.775	7.255	11.199	3.85E+05
29	XE7	7.395	7.456	0.825	7.426	7.997	2.62E+05
30	XF1	6.930	7.023	1.342	6.977	19.786	7.36E+05
31	XF2	7.071	7.163	1.301	7.117	10.037	3.59E+05
32	XF3	7.699	7.737	0.494	7.718	24.384	7.41E+05
33	XF4	7.170	7.192	0.307	7.181	19.559	6.86E+05
34	XF5	6.700	6.748	0.716	6.724	17.240	6.90E+05
35	XF6	8.161	8.161	0.000	8.161	15.891	4.32E+05
36	XF7	7.384	7.771	5.241	7.578	12.505	3.94E+05
37	XG1	7.290	7.316	0.357	7.303	22.254	7.55E+05
38	XG3	6.811	6.911	1.468	6.861	21.185	8.14E+05
39	XG4	6.826	6.961	1.978	6.894	20.684	7.88E+05

40	XG5	6.643	6.838	2.935	6.741	15.781	6.28E+05
41	XG7	7.145	7.158	0.182	7.152	18.672	6.61E+05
42	XH1	7.156	7.252	1.342	7.204	11.279	3.93E+05
43	XH2	7.066	7.270	2.887	7.168	17.372	6.12E+05
44	XH3	7.053	7.242	2.680	7.148	14.290	5.06E+05
45	XH4	7.159	7.257	1.369	7.208	10.588	3.69E+05
46	XH5	7.116	7.159	0.604	7.138	16.099	5.72E+05
47	XH6	7.244	7.507	3.631	7.376	16.813	5.59E+05
48	XH7	6.919	7.044	1.807	6.982	10.998	4.08E+05
49	XI1	6.939	7.006	0.966	6.973	18.183	6.77E+05
50	XI2	6.991	7.036	0.644	7.014	18.405	6.77E+05
51	XI3	7.392	7.446	0.731	7.419	18.566	6.10E+05
52	XI4	7.399	7.443	0.595	7.421	21.613	7.10E+05
53	XI5	6.640	6.658	0.271	6.649	12.401	5.08E+05
54	XI6	7.573	7.586	0.172	7.580	21.674	6.83E+05
55	XI7	7.244	7.413	2.333	7.329	19.003	6.40E+05
56	XJ1	7.294	7.356	0.850	7.325	14.881	5.02E+05
57	XJ2	7.302	7.326	0.329	7.314	13.051	4.41E+05
58	XJ3	6.275	6.453	2.837	6.364	18.631	8.32E+05
59	XJ4	6.919	6.985	0.954	6.952	18.351	6.87E+05
60	XJ5	7.555	7.628	0.966	7.592	20.292	6.37E+05
61	XJ6	7.127	7.252	1.754	7.190	19.790	6.93E+05
62	XJ7	6.836	7.075	3.496	6.956	18.739	7.01E+05
63	XK1	7.198	7.226	0.389	7.212	13.486	4.69E+05
64	XK3	7.825	8.054	2.927	7.940	22.525	6.47E+05
65	XK4	7.013	7.079	0.941	7.046	16.509	6.02E+05
66	XK5	7.423	7.512	1.199	7.468	24.149	7.84E+05
67	XK6	7.124	7.153	0.407	7.139	19.715	7.00E+05
68	XK7	7.334	7.343	0.123	7.339	20.369	6.84E+05
69	XL1	7.229	7.295	0.913	7.262	17.831	6.12E+05
70	XL2	7.191	7.400	2.906	7.296	15.153	5.15E+05
71	XL4	7.384	7.499	1.557	7.442	16.927	5.53E+05
72	XL5	7.394	7.544	2.029	7.469	15.724	5.10E+05
73	XL6	6.999	7.180	2.586	7.090	11.869	4.27E+05
74	XL7	6.886	6.949	0.915	6.918	14.103	5.33E+05
75	XM1	7.538	7.555	0.226	7.547	7.120	2.26E+05
76	XM2	7.147	7.261	1.595	7.204	19.304	6.73E+05
77	XM3	7.024	7.191	2.378	7.108	14.245	5.10E+05
78	XM4	7.376	7.400	0.325	7.388	18.892	6.26E+05
79	XM5	7.389	7.538	2.017	7.464	17.660	5.74E+05
80	XN1	7.133	7.248	1.612	7.191	18.995	6.65E+05
81	XN3	7.477	7.583	1.418	7.530	19.939	6.36E+05
82	XN4	7.297	7.407	1.507	7.352	18.607	6.23E+05
83	XN6	7.017	7.044	0.385	7.031	15.193	5.56E+05
84	XN7	7.088	7.308	3.104	7.198	14.129	4.93E+05

85	XO1	7.935	8.025	1.134	7.980	12.825	3.64E+05
86	XO2	6.946	7.270	4.665	7.108	13.585	4.87E+05
87	XO3	6.847	6.922	1.095	6.885	12.151	4.64E+05
88	XO4	6.962	7.477	7.397	7.220	17.690	6.14E+05
89	XO5	7.053	7.155	1.446	7.104	18.960	6.80E+05
90	XO6	7.286	7.320	0.467	7.303	23.991	8.14E+05
91	XO7	7.592	7.733	1.857	7.663	19.156	5.90E+05
92	RAA208	6.875	6.977	1.484	6.926	19.830	7.48E+05
93	RAA808	7.292	7.305	0.178	7.299	15.103	5.13E+05
94	RAB408	7.211	7.312	1.401	7.262	16.780	5.76E+05
95	RAB908	7.198	7.405	2.876	7.302	18.161	6.16E+05
96	RAC508	6.713	6.828	1.713	6.771	9.085	3.59E+05
97	RAD108	7.537	7.603	0.876	7.570	25.471	8.04E+05
98	RAD508	7.279	7.358	1.085	7.319	21.258	7.18E+05
99	RAE108	7.279	7.358	1.948	7.319	15.853	5.36E+05
100	RAE608	7.279	7.358	1.291	7.319	13.583	4.59E+05
101	RAE208	7.279	7.358	2.710	7.319	16.696	5.64E+05
102	RAF708	7.279	7.358	0.187	7.319	17.517	5.92E+05
103	RAG308	7.279	7.358	0.745	7.319	10.047	3.39E+05
104	RAG808	7.279	7.358	1.061	7.319	10.987	3.71E+05
105	RAH408	7.279	7.358	0.331	7.319	15.761	5.32E+05
106	RAI108	7.279	7.358	1.066	7.319	14.176	4.79E+05
107	RAI608	7.279	7.358	3.491	7.319	19.300	6.52E+05
108	RAJ208	7.279	7.358	0.177	7.319	17.942	6.06E+05
109	RAJ908	7.279	7.358	0.323	7.319	20.192	6.82E+05
110	RAK508	7.279	7.358	1.359	7.319	17.850	6.03E+05
111	RAL208	7.279	7.358	0.529	7.319	18.112	6.12E+05
112	RAL808	7.279	7.358	2.245	7.319	17.288	5.84E+05
113	RAM508	7.279	7.358	2.599	7.319	20.708	7.00E+05
114	RAN208	7.279	7.358	0.767	7.319	13.897	4.69E+05
115	RAN708	7.279	7.358	1.138	7.319	18.863	6.37E+05
116	RAO308	7.279	7.358	3.388	7.319	10.564	3.57E+05
117	RAP108	7.279	7.358	2.186	7.319	18.464	6.24E+05
118	RAP608	7.279	7.358	0.401	7.319	24.034	8.12E+05

(Operator B)

	Sample	Min Diam	Max Diam	% Change	Avg Diam	P(max)	(In PSI) Stress(max)
1	YA1	6.911	6.946	0.506	6.929	15.025	5.66E+05
2	YA2	7.232	7.514	3.899	7.373	24.405	8.12E+05
3	YA3	7.014	7.057	0.613	7.036	17.442	6.38E+05
4	YA4	6.711	6.723	0.179	6.717	13.633	5.47E+05
5	YA5	6.823	6.905	1.202	6.864	16.482	6.33E+05
6	YA6	7.071	7.170	1.400	7.121	14.588	5.21E+05
7	YB1	7.101	7.386	4.014	7.244	16.456	5.67E+05
8	YB2	6.926	7.106	2.599	7.016	8.017	2.95E+05
9	YB3	7.142	7.206	0.896	7.174	17.374	6.11E+05
10	YB4	6.549	6.576	0.412	6.563	17.353	7.29E+05
11	YB5	6.213	6.235	0.354	6.224	13.043	6.09E+05
12	YB6	7.153	7.177	0.336	7.165	17.007	5.99E+05
13	YC1	7.210	7.400	2.635	7.305	15.090	5.12E+05
14	YC2	7.289	7.355	0.905	7.322	18.204	6.14E+05
15	YC3	7.070	7.219	2.107	7.145	15.411	5.46E+05
16	YC4	6.786	6.797	0.162	6.792	16.561	6.50E+05
17	YC5	7.275	7.369	1.292	7.322	19.653	6.63E+05
18	YC6	7.165	7.232	0.935	7.199	12.793	4.47E+05
19	YD1	6.728	6.866	2.051	6.797	14.950	5.86E+05
20	YD2	6.994	7.107	1.616	7.051	21.575	7.85E+05
21	YD3	6.846	6.895	0.716	6.871	20.377	7.81E+05
22	YD4	7.399	7.405	0.081	7.402	18.421	6.08E+05
23	YD6	7.002	7.202	2.856	7.102	18.914	6.78E+05
24	YE1	7.344	7.498	2.097	7.421	15.106	4.96E+05
25	YE2	7.554	7.794	3.177	7.674	20.417	6.27E+05
26	YE3	7.119	7.506	5.436	7.313	11.417	3.86E+05
27	YF1	7.101	7.175	1.042	7.138	20.259	7.19E+05
28	YF2	7.249	7.277	0.386	7.263	17.593	6.03E+05
29	YF3	7.455	7.495	0.537	7.475	25.341	8.21E+05
30	YF4	7.479	7.592	1.511	7.536	20.683	6.59E+05
31	YG1	7.561	7.637	1.005	7.599	20.471	6.41E+05
32	YH2	6.703	6.718	0.224	6.711	17.293	6.95E+05
33	YH3	7.213	7.247	0.471	7.230	18.693	6.47E+05
34	YH4	7.224	7.267	0.595	7.246	14.779	5.09E+05
35	YH5	6.950	7.065	1.655	7.008	19.397	7.15E+05
36	YH6	7.082	7.191	1.539	7.137	17.105	6.08E+05
37	YI1	7.204	7.465	3.623	7.335	6.666	2.24E+05
38	YI2	7.191	7.443	3.504	7.317	18.599	6.29E+05
39	YI3	6.706	6.723	0.254	6.715	14.454	5.80E+05
40	YI4	7.353	7.456	1.401	7.405	14.973	4.94E+05
41	YI6	6.653	6.958	4.584	6.806	6.393	2.50E+05
42	YI7	6.934	7.092	2.279	7.013	15.657	5.76E+05

43	YJ1	7.226	7.330	1.439	7.278	20.588	7.03E+05
44	YJ2	7.330	7.437	1.460	7.384	15.899	5.28E+05
45	YJ3	6.240	6.335	1.522	6.288	12.327	5.64E+05
46	YJ4	7.720	7.823	1.334	7.772	11.169	3.35E+05
47	YJ5	7.537	7.560	0.305	7.549	20.661	6.56E+05
48	YJ6	7.672	7.735	0.821	7.704	16.471	5.02E+05
49	YJ7	7.563	7.669	1.402	7.616	14.892	4.65E+05

AS4-019 DATA
(Operator A)

	Sample	Min Diam	Max Diam	% Change	Avg Diam	Failure Load (gms)	Failure Stress (psi)
1	AA1	6.469	6.599	2.010	6.534	11.928	5.06E+05
2	AA2	6.933	6.994	0.880	6.964	2.847	1.06E+05
3	AA3	7.552	7.561	0.119	7.557	20.406	6.47E+05
4	AA4	6.891	7.006	1.669	6.949	16.617	6.23E+05
5	AA5	6.738	6.890	2.256	6.814	17.704	6.90E+05
6	AB1	7.532	7.591	0.783	7.562	19.693	6.23E+05
7	AB2	6.990	7.193	2.904	7.092	14.305	5.15E+05
8	AB3	6.924	6.925	0.014	6.925	19.350	7.30E+05
9	AB4	6.907	6.974	0.970	6.941	18.836	7.08E+05
10	AB5	7.036	7.142	1.507	7.089	14.332	5.16E+05
11	AC1	7.145	7.281	1.903	7.213	16.600	5.77E+05
12	AC2	6.582	6.716	2.036	6.649	18.619	7.62E+05
13	AC3	6.621	6.642	0.317	6.632	13.267	5.46E+05
14	AC4	8.015	8.054	0.487	8.035	18.412	5.16E+05
15	AC5	7.003	7.048	0.643	7.026	17.244	6.32E+05
16	AC6	6.643	6.748	1.581	6.696	9.865	3.98E+05
17	AC7	6.520	6.610	1.380	6.565	15.872	6.66E+05
18	AD1	7.245	7.397	2.098	7.321	10.486	3.54E+05
19	AD2	6.767	6.802	0.517	6.785	14.416	5.67E+05
20	AD3	7.251	7.259	0.110	7.255	7.292	2.51E+05
21	AD4	7.207	7.263	0.777	7.235	18.173	6.28E+05
22	AD5	7.486	7.613	1.697	7.550	18.707	5.94E+05
23	AD6	6.289	6.508	3.482	6.399	8.208	3.63E+05
24	AE1	6.795	7.038	3.576	6.917	12.626	4.78E+05
25	AE2	7.031	7.474	6.301	7.253	16.841	5.79E+05
26	AE3	7.114	7.435	4.512	7.275	20.961	7.17E+05
27	AE4	6.828	6.895	0.981	6.862	17.682	6.80E+05
28	AE5	6.616	6.712	1.451	6.664	15.385	6.27E+05
29	AE6	6.371	6.493	1.915	6.432	13.193	5.77E+05
30	AE7	7.291	7.323	0.439	7.307	11.231	3.81E+05
31	AE8	6.553	6.763	3.205	6.658	16.877	6.89E+05
32	AF1	6.887	6.908	0.305	6.898	12.507	4.76E+05
33	AF2	7.135	7.207	1.009	7.171	15.037	5.29E+05
34	AF3	7.231	7.240	0.124	7.236	16.960	5.86E+05
35	AF4	7.494	7.501	0.093	7.498	14.649	4.72E+05
36	AG1	7.016	7.035	0.271	7.026	12.098	4.43E+05
37	AG2	6.644	6.827	2.754	6.736	17.047	6.80E+05
38	AG3	6.896	6.928	0.464	6.912	17.607	6.67E+05
39	AG4	7.165	7.193	0.391	7.179	15.951	5.60E+05
40	AG5	6.934	6.935	0.014	6.935	16.248	6.11E+05
41	AH3	6.874	7.254	5.528	7.064	16.913	6.13E+05

42	AH4	6.923	6.977	0.780	6.950	16.703	6.26E+05
43	AI2	6.949	7.366	6.001	7.158	13.205	4.66E+05
44	AI3	5.829	5.829	0.000	5.829	12.163	6.48E+05
45	AI4	7.288	7.366	1.070	7.327	20.725	6.98E+05
46	AI5	7.229	7.405	2.435	7.317	14.702	4.97E+05
47	AJ1	6.847	6.955	1.577	6.901	18.945	7.20E+05
48	AJ2	7.077	7.181	1.470	7.129	17.810	6.34E+05
49	AJ3	7.175	7.385	2.927	7.280	20.243	6.91E+05
50	AJ4	6.535	6.702	2.555	6.619	13.892	5.74E+05
51	AJ5	6.788	6.877	1.311	6.833	12.017	4.66E+05
52	AJ6	7.022	7.062	0.570	7.042	12.487	4.56E+05
53	AK1	6.581	6.852	4.118	6.717	16.248	6.52E+05
54	AK2	7.099	7.130	0.437	7.115	20.105	7.19E+05
55	AK4	7.746	7.837	1.175	7.792	20.440	6.09E+05
56	AK5	6.967	6.972	0.072	6.970	14.434	5.38E+05
57	AK6	7.235	7.399	2.267	7.317	15.602	5.27E+05
58	AL1	7.179	7.188	0.125	7.184	13.491	4.73E+05
59	AL2	6.725	6.917	2.855	6.821	11.448	4.45E+05
60	AL3	7.359	7.363	0.054	7.361	10.775	3.60E+05
61	AL4	6.731	6.995	3.922	6.863	13.871	5.33E+05
62	AL6	7.021	7.123	1.453	7.072	17.252	6.24E+05
63	AL7	6.648	6.791	2.151	6.720	14.676	5.88E+05
64	AM1	7.685	7.768	1.080	7.727	14.002	4.24E+05
65	AM2	7.797	7.845	0.616	7.821	17.149	5.07E+05
66	AM3	7.044	7.165	1.718	7.105	10.615	3.81E+05
67	AM5	6.864	6.981	1.705	6.923	14.825	5.60E+05
68	AM6	7.553	7.850	3.932	7.702	17.996	5.49E+05
69	AM7	7.044	7.075	0.440	7.060	11.812	4.29E+05
70	AN1	7.355	7.537	2.475	7.446	19.475	6.36E+05
71	AN2	7.609	7.816	2.720	7.713	20.150	6.13E+05
72	AN3	7.356	7.375	0.258	7.366	20.665	6.89E+05
73	AN4	7.328	7.461	1.815	7.395	13.889	4.60E+05
74	AN5	6.828	6.856	0.410	6.842	17.528	6.77E+05
75	AN6	7.114	7.158	0.618	7.136	20.331	7.22E+05
76	AN7	7.797	7.801	0.051	7.799	20.269	6.03E+05
77	AO1	7.315	7.456	1.928	7.386	20.594	6.83E+05
78	AO2	7.694	7.746	0.676	7.720	23.191	7.04E+05
79	AO3	7.118	7.393	3.863	7.256	13.424	4.61E+05
80	AO4	7.191	7.477	3.977	7.334	18.601	6.26E+05
81	AO5	7.985	8.010	0.313	7.998	17.955	5.08E+05
82	AO6	7.017	7.073	0.798	7.045	22.246	8.11E+05
83	AP1	7.329	7.407	1.064	7.368	17.082	5.69E+05
84	AP2	7.003	7.006	0.043	7.005	17.133	6.32E+05
85	AP3	7.159	7.398	3.338	7.279	19.336	6.60E+05
86	AP4	7.330	7.779	6.126	7.555	18.056	5.72E+05

87	AP5	7.154	7.217	0.881	7.186	20.128	7.05E+05
88	AP6	6.513	6.547	0.522	6.530	19.093	8.10E+05
89	AQ1	7.305	7.461	2.136	7.383	15.744	5.23E+05
90	AQ2	6.822	6.860	0.557	6.841	20.400	7.89E+05
91	AQ3	7.440	7.510	0.941	7.475	20.120	6.52E+05
92	AQ4	6.702	6.736	0.507	6.719	10.494	4.21E+05
93	AQ5	7.062	7.174	1.586	7.118	19.046	6.80E+05
94	AQ6	7.483	7.620	1.831	7.552	14.485	4.60E+05
95	AQ7	7.003	7.004	0.014	7.004	15.852	5.85E+05
96	AR1	7.608	7.687	1.038	7.648	17.501	5.41E+05
97	AR2	7.290	7.468	2.442	7.379	18.495	6.15E+05
98	AR3	6.785	6.796	0.162	6.791	6.628	2.60E+05
99	AR4	6.658	6.939	4.220	6.799	16.452	6.44E+05
100	AR5	6.959	7.077	1.696	7.018	10.663	3.92E+05
101	AR6	6.383	6.479	1.504	6.431	15.041	6.58E+05
102	AR7	8.323	8.500	2.127	8.412	18.513	4.73E+05
103	AS1	7.160	7.176	0.223	7.168	17.802	6.27E+05
104	AS2	7.015	7.069	0.770	7.042	10.802	3.94E+05
105	AS3	7.207	7.306	1.374	7.257	16.084	5.53E+05
106	AS4	6.808	6.876	0.999	6.842	12.678	4.90E+05
107	AS5	7.017	7.161	2.052	7.089	10.226	3.68E+05
108	AS6	6.668	6.718	0.750	6.693	15.287	6.17E+05
109	AS7	7.559	7.596	0.489	7.578	22.836	7.20E+05
110	AT1	6.984	7.086	1.460	7.035	18.146	6.63E+05
111	AT2	7.174	7.250	1.059	7.212	19.507	6.79E+05
112	AT3	7.119	7.211	1.292	7.165	6.700	2.36E+05
113	AU1	6.902	7.038	1.970	6.970	15.632	5.82E+05
114	AU2	7.340	7.422	1.117	7.381	15.841	5.26E+05
115	AU3	6.464	6.577	1.748	6.521	20.860	8.88E+05
116	AV1	7.203	7.224	0.292	7.214	16.858	5.86E+05
117	AV2	7.204	7.395	2.651	7.300	7.643	2.60E+05
118	AV3	7.474	7.690	2.890	7.582	6.607	2.08E+05
119	AW1	7.087	7.113	0.367	7.100	15.356	5.51E+05
120	AW2	7.171	7.910	10.305	7.541	16.096	5.12E+05
121	AW3	7.360	7.450	1.223	7.405	18.932	6.25E+05

AS4-019 DATA
(Operator B)

	Sample	Min Diam	Max Diam	% Change	Avg Diam	Failure Load (gms)	Failure Stress (psi)
1	BAA3	7.299	7.450	2.069	7.375	14.481	4.82E+05
2	BAA4	6.722	7.031	4.597	6.877	19.433	7.44E+05
3	BAA5	6.981	6.983	0.029	6.982	13.484	5.00E+05
4	BAA6	7.054	7.083	0.411	7.069	18.118	6.56E+05
5	BAA7	8.003	8.201	2.474	8.102	23.177	6.39E+05
6	BAA8	7.736	7.861	1.616	7.799	18.561	5.52E+05
7	BBB1	7.530	7.647	1.554	7.589	17.757	5.58E+05
8	BBB2	7.242	7.253	0.152	7.248	18.883	6.50E+05
9	BBB3	7.319	7.498	2.446	7.409	14.346	4.73E+05
10	BBB4	6.652	6.880	3.428	6.766	16.350	6.46E+05
11	BBB5	6.971	7.089	1.693	7.030	16.685	6.11E+05
12	BBB6	6.640	6.658	0.271	6.649	18.452	7.55E+05
13	BCC1	7.149	7.450	4.210	7.300	12.469	4.23E+05
14	BCC2	7.622	7.737	1.509	7.680	20.320	6.23E+05
15	BCC3	7.090	7.107	0.240	7.099	9.753	3.50E+05
16	BCC4	6.349	6.583	3.686	6.466	16.735	7.24E+05
17	BCC5	6.973	7.078	1.506	7.026	17.848	6.54E+05
18	BDD2	6.998	7.021	0.329	7.010	14.596	5.38E+05
19	BDD3	7.137	7.161	0.336	7.149	18.166	6.43E+05
20	BDD4	7.085	7.097	0.169	7.091	17.677	6.36E+05
21	BDD5	6.993	7.011	0.257	7.002	14.855	5.48E+05
22	BDD6	7.278	7.325	0.646	7.302	20.191	6.85E+05
23	BDD7	6.565	6.933	5.605	6.749	9.624	3.82E+05
24	BA1	7.336	7.560	3.053	7.448	14.353	4.68E+05
25	BA3	7.175	7.175	0.000	7.175	13.616	4.79E+05
26	BB1	6.991	7.052	0.873	7.022	13.834	5.08E+05
27	BB2	7.431	7.558	1.709	7.495	20.251	6.52E+05
28	BB4	7.601	7.655	0.710	7.628	14.929	4.64E+05
29	BC1	7.630	7.756	1.651	7.693	15.278	4.67E+05
30	BC2	6.871	6.876	0.073	6.874	12.614	4.83E+05
31	BC3	6.953	6.972	0.273	6.963	13.562	5.06E+05
32	BC4	6.870	6.940	1.019	6.905	17.508	6.64E+05
33	BC5	6.568	6.705	2.086	6.637	15.954	6.55E+05
34	BD1	7.101	7.183	1.155	7.142	20.928	7.42E+05
35	BD2	7.245	7.408	2.250	7.327	19.327	6.51E+05
36	BD4	6.986	7.120	1.918	7.053	18.217	6.63E+05
37	BE1	7.522	7.729	2.752	7.626	14.069	4.38E+05
38	BE2	6.807	6.899	1.352	6.853	10.342	3.98E+05
39	BE4	7.710	7.807	1.258	7.759	23.890	7.18E+05
40	BE6	7.766	7.788	0.283	7.777	17.320	5.18E+05
41	BE7	7.164	7.353	2.638	7.259	17.686	6.07E+05

REFERENCES

1. Weibull, W. "A Statistical Distribution Function of WideApplicability," Journal of Applied Mechanics, (Sep 1951) pp. 293-7.

2. Metcalfe, A. G. and Schmitz, G. K., "Effect of Length on the Strength of Glass Fibers," Americal Society for Testing and Materials Proceedings, Vol. 64 (1964) pp. 1075-93.

3. Rosen, B. M., "Tensile Failure of Fibrous Composites," AIAA Journal, Vol. 2, No. 11 (Nov 1964) pp.1985-91.

4. Daniels, H. E., "The Statistical Theory of the Strength of Bundles of Threads," Prodeedings of the Royal Society (London), Vol. 183A (1945) pg 405.

5. Zweben, C. and Rosen, B. M., "Tensile Failure Criteria for Fiber Composite Materials," NASA CR-2057 (Aug 1972).

6. Harlow, D. G. and Phoenix, S. L., "The Chain-of-Bundles Probability Model for Strength of Fibrous Materials I: Analysis and Conjectures," J. Composite Materials, Vol. 12 (Apr 1978), pp 195-214.

7. Harlow, D. G. and Phoenix, S. L., "The Chain-of-Bundles Probability Model for Strength of Fibrous Materials II: Analysis and Conjectures," J. Composite Materials, Vol. 12 (Jul 1978), pp 314-34.

8. Bell, D.K., "Composite Reliability Enhancement via Preloading," Masters Thesis, Naval Post Graduate School, Monterey, Ca (Sep 1986) pp 57-61.

9. Bury, K. V., "Statistical Models in Applied Science," Wiley Series in Probability and Mathematical Statistics. New York; John Wiley & Sons.

10. Kunkel, J. S., "Effect of fiber Diameter on the Reliability of Composites - Automated Laser Diffraction Implementation," Masters Thesis, Naval Post Graduate School, Monterey, Ca (Dec 1987) pp 15-18, 30-34.

11. Kapur, K. C. and Lamberson, L. R., "reliability in Engineering Design," John Wiley & Sons Inc., New York, 1977.

12. Wu, E. M., Internal Report, Naval Post Graduate School, Monterey, Ca.

13. Goeke, E. C. and Chou, S. C., "Examination of the Tensile Strength of Graphite Fibers," US Army Laboratory Command MTL TR 89-16 (Feb 1989).

14. Bennet, T. A., "A Comparison of Two Methods for Fiber Diameter Measurement and a System Design for the Study of Composite Reliability," Masters Thesis, Naval Post Graduate School, Monterey, Ca (Dec 1985).

15. Storch, M. G., "A Computer Aided Method for the measurement of Fiber Diameters by Laser Diffraction," Masters Thesis, Naval Post Graduate School, Monterey, Ca (Sep 1986).

INITIAL DISTRIBUTION LIST

	No. Copies
1. Defense Technical Information Center Cameron Station Alexandria, VA 22314-6145	2
2. Library, Code 0142 Naval Postgraduate School Monterey, CA 93943-5100	2
3. Department Chairman Department of Aeronautics and Astronautics Naval Postgraduate School Monterey, CA 93943-5000	2
4. Professor Ed Wu, Code 67WT Department of Aeronautics and Astronautics Naval Postgraduate School Monterey, CA 93943-5000	5
5. Lcdr Carl Engelbert Harrier Det London Box 75 FPO New York, NY 09510-1900	3